Exploring morphological variation of Rough periwinkle *(Littorina saxatilis)* shells along exposed and sheltered rocky shores, with three data transformation methods

INTRODUCTION

Rocky shore is a spatially and temporally heterogeneous environment (Witman, 1985; Helmuth and Hoffman, 2001). Gastropod mollusc morphology, concentrating on shape, size, and colour of the shell and size of the foot (Clarke et al., 1998; Trussell 1997, Reimchen, 1974), shell strength (Vermeij and Currey, 1980) can be used for modelling strategies of adaptation to such environment on a small (De Wolf et al., 1997; Sundberg, 1988) and also large geographic scale (Etter, 1988; Trussell 2000).

Phenotypic plasticity (Agrawal, 2001) can lead to different ecotypes as a result of local adaptation (Hollander et at., 2006; Janson, 1982). *Littorina saxatilis* is one of the most polymorphic species of winkles, having different ecotypes based on their shell morphology, predators and distribution on sea shores (Figure 1, Table 1; Reid, 1996; Hull et al., 1996; Johannesson, 2003).

Figure 1. The morphological variation (aperture area, thickness of shell) in *L. saxatilis* along sea shores are suggested to be mainly correlated with wave action and crab predation in several countries (Johannesson, 2003)

Morphological constraint on coiled shells can be explained mathematically (Raup, 1961; Vermeij, 1971; Kemp and Bertness, 1984). The aperture growth determines the overall shell form and snail foot size (Trussell, 1997), so it is one of the main morphological shell character. Whorl expansion and apical angle are also main factors generating the great variety of shells in *L. saxatilis* and *L. arcana* (Clarke et al., 1999; Thompson, 1942).

Environmental conditions, such as wave action (risk of dislodgement, Trussell et al., 1993), can force a shift in the covariation between several traits (Grahame and Mill, 1986; Trussell, 1977; Heller, 1976). This leads to an overall change in morphology. Therefore, when considering shell morphology it is important to use covariate matrixes, not singular features (Schindel, 1990; Béguinot, 2014).

Table 1. Many *L. saxatilis* ecotypes have been identified in different countries. These studies mostly concentrate on wave exposure and crab predation leading to shape variation. However, biologically important factors (e.g. sexual maturity and accommodating brood)should also be consider (Walker and Grahame, 2011; Conde-Padin et al., 2007 and 2009).

L. saxatilis ecotype	Description	Country	Reference
Moderate	Moderately exposed boulder shores, relatively large (>10mm), thick and the aperture is relatively narrow	UK	Reid, 1996
Wave-exposed	Exposed shores, less crab predation more exposed to dislodgement, smaller in size (4-6 mm), thin-walled, larger foot, larger aperture	UK	Reid, 1996
Barnacle	Globular in shape, dark in colour and very small in size (<3mm)	UK	Johannesson, 2003
H	On large boulders (3-4m diameter), in the upper part of the intertidal zone	UK	Hull et al., 1996; Johannesson, 2003
M	On moderately sizes boulders (1-2m) in the mid-intertidal zone	UK	Hull et al., 1996; Johannesson, 2003
RB	Ridged and banded, associated with the barnacle belt from the mid to upper shore, twice the size than SU	Spain	Johannesson et al., 1993; Johannesson et al., 1995
SU	Smooth and unbanded, in the mussel belt from mid to lower shore, aperture size SU>RB	Spain	Johannesson et al., 1993; Johannesson et al., 1995
E	Large aperture, thin shell	Sweden	Jason and Sundberg, 1983
S	Smaller aperture and thick shell	Sweden	Jason and Sundberg, 1983
I	Between E and S for few meters	Sweden	Jason and Sundberg, 1983

The aim of this study was to (1) look for morphological changes in shells of *L. saxatilis* between sheltered versus exposed rocky shores with Principal Component Analysis (PCA) and (2) to explore if ratios of measurements or (3) the transformation methods applied by Clarke at al. (1999) capture the morphological variation more efficiently. With a combination of multivariate statistical methods, detailed shape differences were explored.

MATERIALS

We collected *L. saxatilis* specimens from two transects, 20 meter long each, at two different sites at Combe Martin beach in North Devon on 24 March, 2017. Site A (51°12'29.6"N 4°02'24.8"W) was exposed, described by flat rock surface and, site B (51°12'27.7"N 4°02'24.7"W) was a sheltered area, alongside a rock face, with many crevices and rock pools (Figure 2). We collected all winkles at two meter interval within a 1 m^2 area along transects (n_A=128, n_B=79). Control group consisted of ten flat periwinkle *(L. obtusata)* shells collected at Watermouth beach (Site C, 51°12'56.9"N 4°04'27.8"W) and one dog whelk (Site
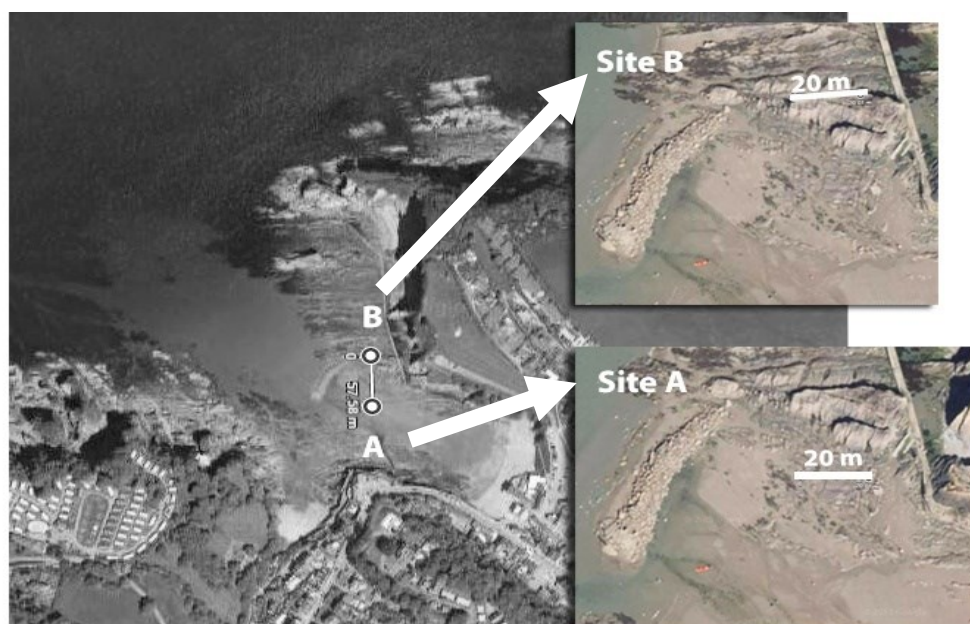

Figure 2. Sampling at Combe Martin beach, North Devon. Site A was moderately exposed as there was a man-made sea defence. Site B was alongside a rock face, providing shelter for organisms. Site A was 57.6 m away from site B. Satellite images from Google Maps.

B, *Nucella lapillus).* Samples were measured using a digital calliper recording Madec and Bellido's (2007) measurements (Figure 3) with 0.1 mm accuracy. Measuring was uniform as one student measured constantly two characters and then the following student measured the next two measurements of each shell. Data was directly put into an Excel data sheet. For each sampling station along transects, we truncated sample size at 20 winkles.

Figure 3. One 20 m transect was used per site, periwinkles were collected at 2m intervals. The scales on the photographs are representatives of 1 cm. The exact locations of the samples were recorded with pencil and placed in the sample tubes. Molluscs often use crevices, holes and surface irregularities as shelters against environmental stressors (Pardo and Johnston, 2004).

MULTIVARIATE METHODS AND OUTCOMES

Littorina saxatilis shape differences on exposed versus sheltered shores were investigated using (1) Principal Component Analysis (PCA, normal and Bayesian, Table 2), (2) Cluster Analysis (CLA, hierarchical and model based, the latter not discussed in this paper, Fraley and Raftery, 1998) and (3) Nonmetric Multidimensional Scaling (NMDS). General terms and approaches are described by Paily and Shankar (2016) (Table 3).

Table 2. Several mathematical changes can be applied to PCA and in the last decade, many PCAs have been developed for different data sets.

PCA name	References
Probabilistic PCA	Tippings and Bishop, 1999
Partially Bayesian PCA	Nakajima et al., 2011
Fully Bayesian	Bishop, 1999
Multiscale PCA	Bakshi, 1995
Maximum likelihood PCA	Wentzell et al., 1997
Exponentially weighted moving PCA	Wold, 1994
Bayesian PCA	Nounou et al., 2002

Table 3. The three multivariate analysis used in this paper and their description and drawbacks.

Analysis	Data matrix	Assumed relationship	Description	Output	Drawbacks	References
PCA	Orthogonal sparse coefficient matrix in Euclidian distance	Linear	It operates within orthogonal sparse coefficient matrix, one containing transformed variables (scores) and the other matrix containing the new axes of rotation (loadings) retaining the most variation in the original data. The loadings maximize the variations found by the PCA.	Represents the largest gradient of variability in the data set decreases on the different PC axes. The distribution of objects correspond to the similarity of the variable's scores.	Information about range of variation and the mean value of PC loading and scores is not available.	Pearson, 1901; Paily and Shankar, 2016; Abdi and Williams, 2010
NMDS	Dissimilarity matrix in Euclidian distance	Any	A small number of ordination axes are chosen prior to the analysis and the data is fitted to those dimensions. It ranks the distances among all distances and then it finds N-dimensional ordination space that best matches differences in ranks.	A 'map', representing ranks of pairwise dissimilarities among objects.	Not an eigenvector-based gradient analysis but it is used for graphical representation. It also loads all variance onto the two axes, and it is easier to see but does not provide information of variable contributions.	Kenkel and Orloci, 1986; Rabinowitz, 1975; Paily and Shankar, 2016
CLA	Matrix of observations and objects in Euclidian distance	Any	Computes multiscale bootstrap resampling to calculate p-values for each cluster after hierarchical clustering.	For a cluster with AU p-value > 0.05, Clusters with AU larger than 95% are highlighted by rectangles, which are strongly supported by data.	Hard to tell how correct a cluster is supported by the data. It can be used only for visualisation.	Suzuki and Shimodaira, 2006 and 2004; Shimodaira, 2004 and 2002

The analyses were performed on the three different data sets ($\log_e$ transformed, ratios, geometric mean transformed), separately for exposed, sheltered and the combination of the two (Figure 4). Normal PCA was performed in Multivariate Statistical Package (MVSP 3.1, Kovach 1999), the other methods were carried out in R 3.4.0 (R scripts, raw data available on WinkleStats, 2017). See data
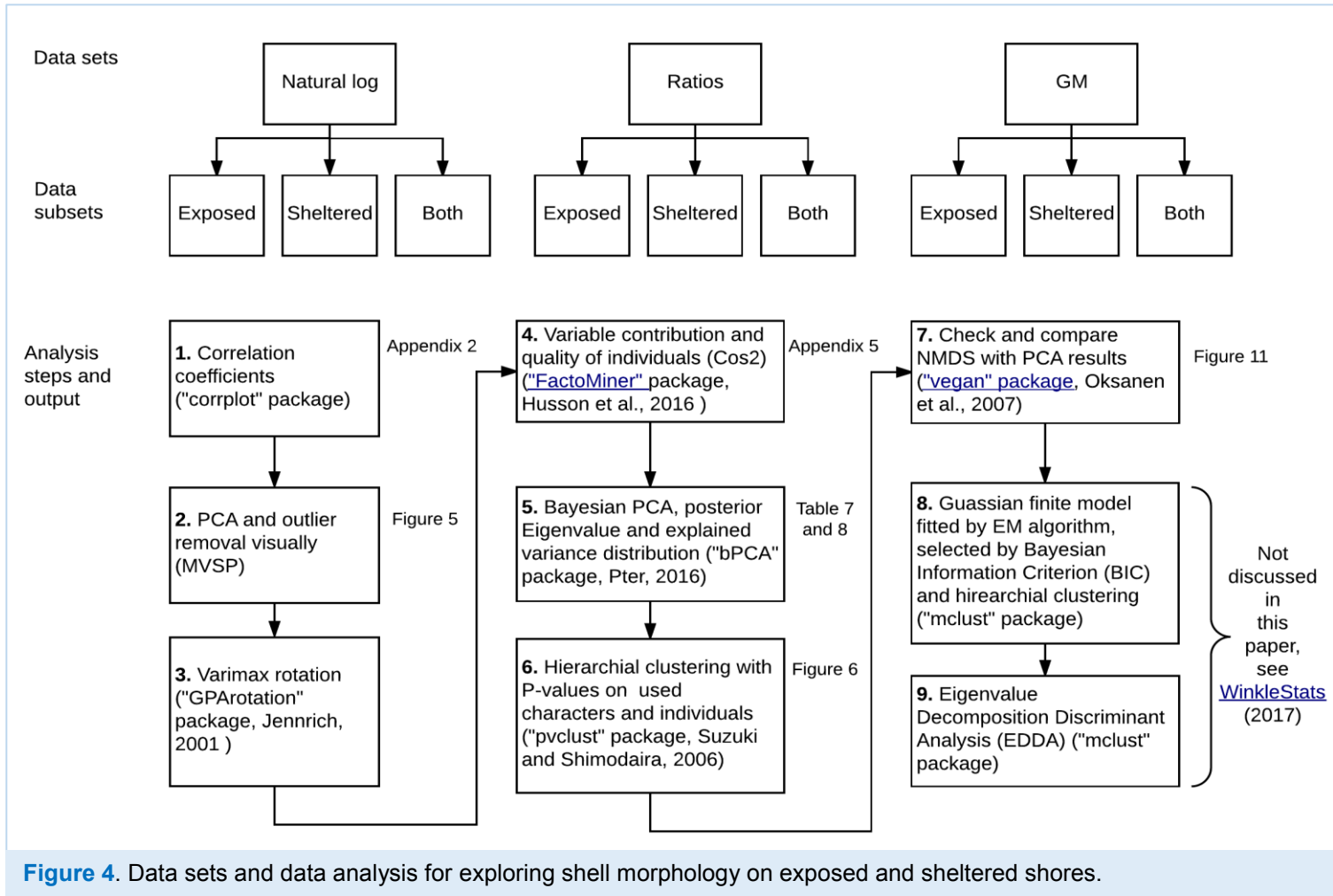

Figure 4. Data sets and data analysis for exploring shell morphology on exposed and sheltered shores.

1. PCA on log transformed raw data

Continuous raw data showed linear relationship between the measurements. This linear relationship justified using PCA (Paily and Shankar, 2016). First, preforming centred PCA (Abdi and Williams, 2010) on our original data (n_A=128, n_B=79) of measurements with $\log_{e\text{-}}$ transformation, six outliers were identified with a scatterplot (B.12, B.20, B37, and FW.5, FW. 6) and were removed. Axis 1 contributed 96.12% of the variance, and consisted of only positive loadings,

followed by 1.504% (Axis 2) and the residual 2.376% was explained by the remaining four axes (Table 4). The control group was identified easily with the PCA, forming a cluster (Figure 5). This was removed for calculating PCA loadings. Spearman correlation between the raw variables were all positive and significant (P<0.001 in all cases) which did not add new information.

Table 4. Results of PCA on $\log_e$ transformed measurements excluding outliers and the control group. On axes 1 and 2, all variables show significant variable loadings (shown in bold, <± 0.1).

| PCA variable loadings	Axis 1	Axis 2	Axis 3	Axis 4	Axis 5	Axis 6
ln BE	**0.334**	**0.11**	**0.906**	**0.206**	-0.034	**-0.109**
ln EF	**0.434**	**-0.893**	-0.063	0	-0.072	-0.076
ln FG	**0.427**	**0.273**	**-0.11**	**-0.477**	**-0.709**	-0.015
ln CD	**0.408**	**0.241**	**-0.372**	**0.784**	**-0.129**	-0.074
ln AB	**0.407**	**0.212**	**-0.154**	**-0.311**	**0.572**	**-0.585**
ln BG	**0.432**	**0.113**	-0.031	**-0.137**	**0.383**	**0.797**
Eigenvalues	1.223	0.019	0.015	0.009	0.005	0.001
Percentage	96.12	1.504	1.185	0.684	0.393	0.114
Cum. Percentage	96.12	97.624	98.81	99.493	99.886	100
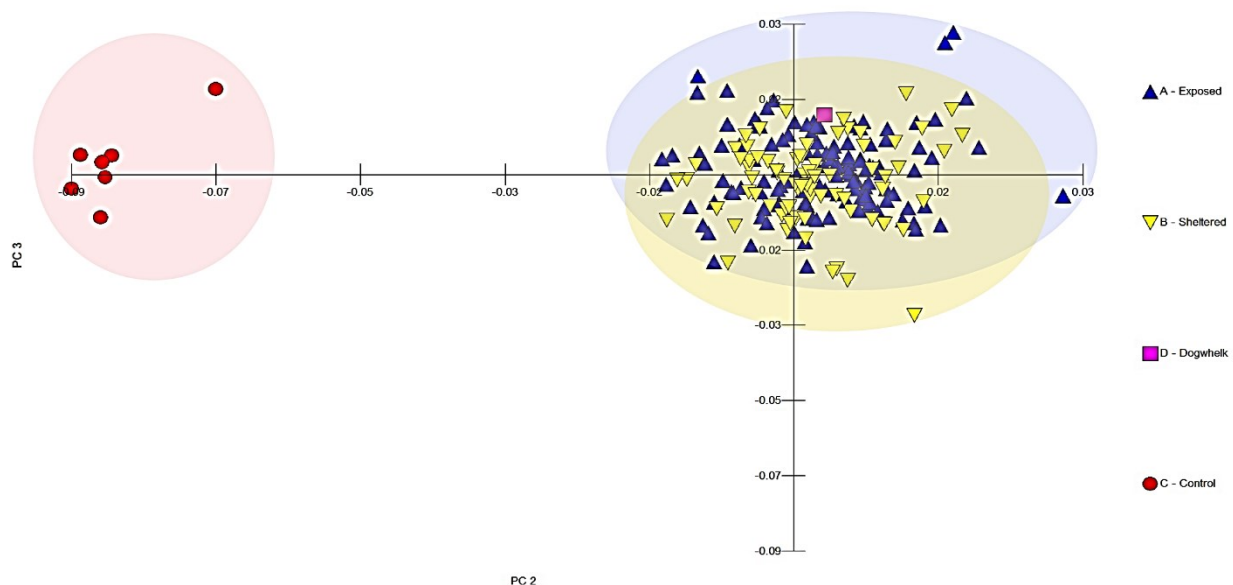
Figure 5. Axis 2 and 3 showing PCA results. These axes show morphological differences. The control group (red circles) is a clearly identified cluster. The exposed (blue triangle) and sheltered (yellow upside down triangle) overlap greatly. The dogwhelk (pink square) sits in the overlapping area.

Hierarchical clustering of Euclidian distance matrices of the $\log_e$ transformed data was performed with P-values via multiscale bootstrap resampling with "pvclust" R package (Figure 6, Suzuki and Shimodaira, 2006). The average clustering showed that based on P-values total width (AB), total height (BG) and aperture width (FG) are the most correlated measurements. As the PCA showed that 95.308% of the variation is explained by axis 1 and the total width and height are the most significant measurements according to the cluster analysis, it is justified that axis 1 is associated with size.
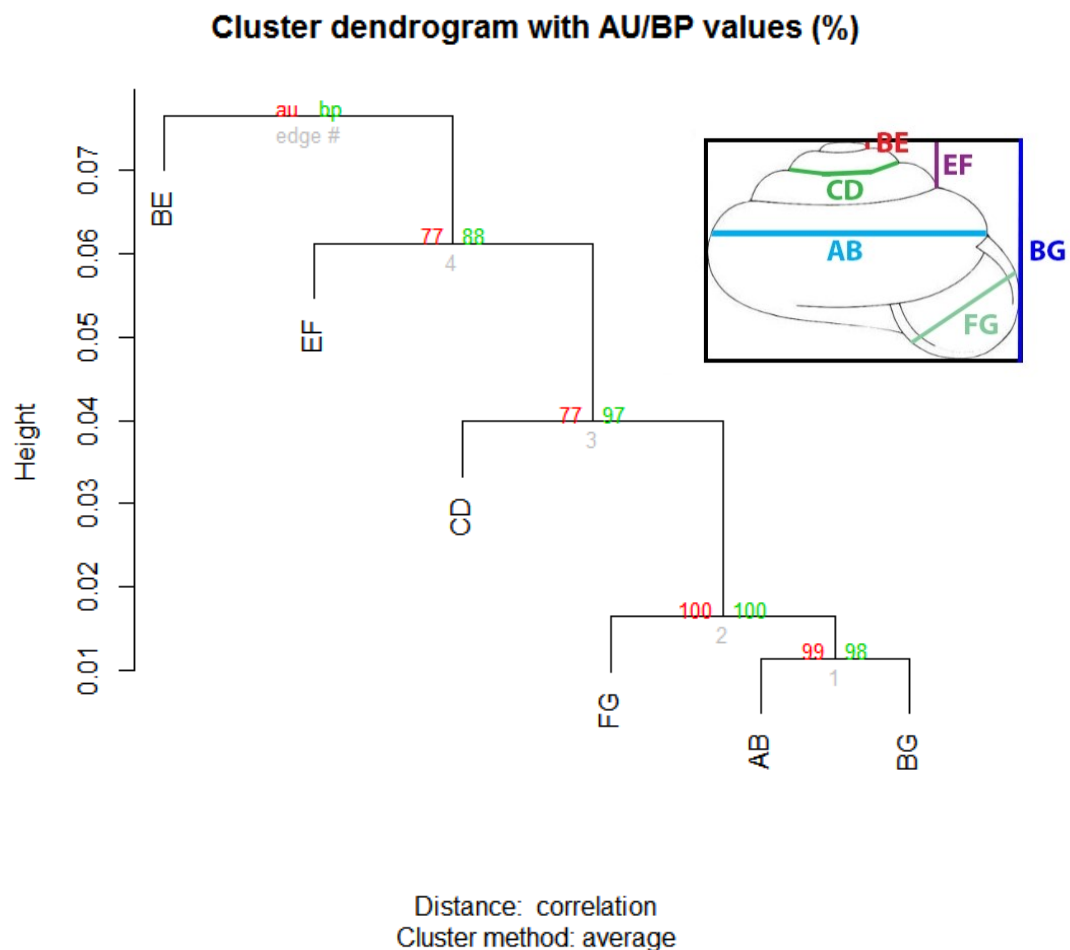

Figure 6. Hierarchical clustering with P-values via multiscale bootstrap resampling. Bootstrapping was set to 1000. AB (total width) and BG (total height) and FG (aperture width) are the most significant with high AU (Approximately Unbiased) and BP (Bootstrap Probability) P-values. These characters are highly correlated.

Enhanced hierarchical clustering with the hclust() function ("fastcluster" package), the individual shells were clustered according to their distribution (exposed vs sheltered, Figure 7) with a node a showing a mixture of the two. The PCA and CLA is showing clear difference between the sizes of the shells on the two sites.
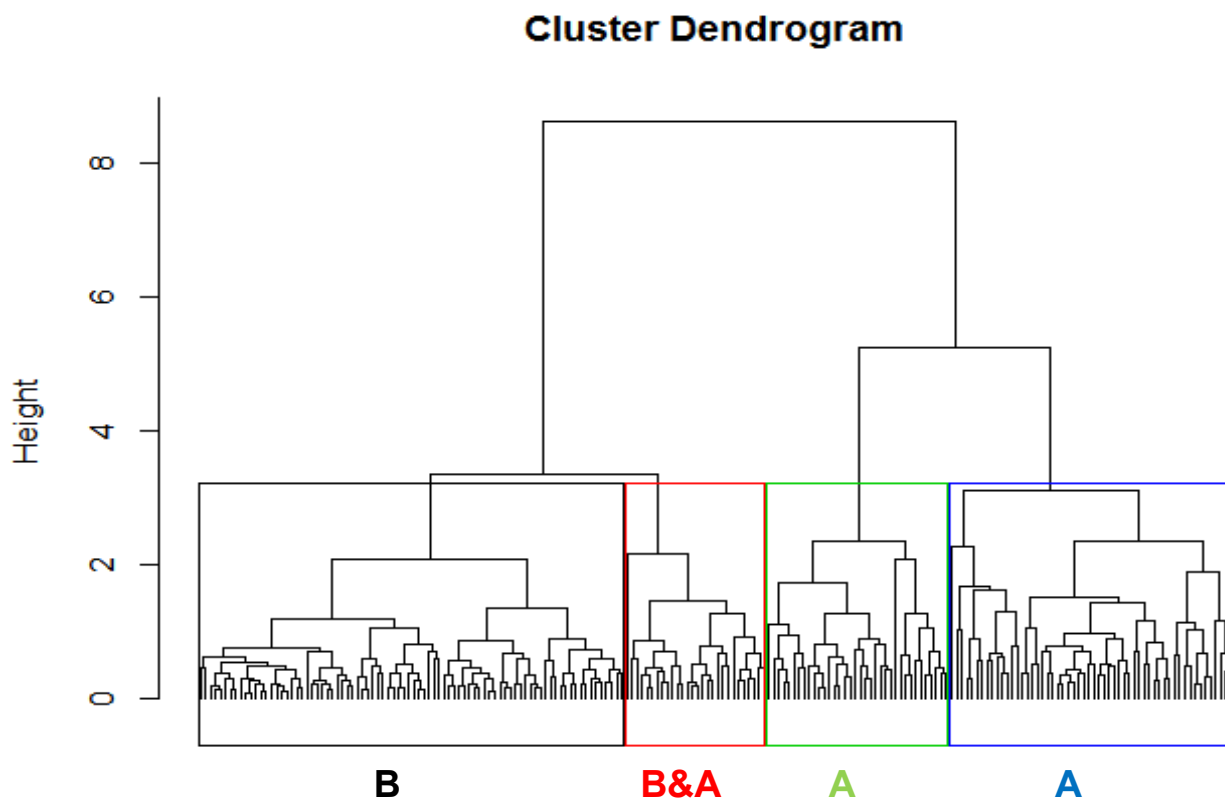
Cluster Dendrogram

Figure 7. Enhanced hierarchical clustering in Euclidian pairwise distance matrices separating exposed (A) and sheltered (B) sites. Sample ID labels were removed for clearer representation. When performed on raw data, outliers were identified again.

2. Normal PCA on ratios of measurements

The aim of performing PCA on ratios between measurements was to test if this data set can show a more clear difference between shell morphology on the two different shores, as shown in other studies (e.g. Grahame and Mill, 1989; Smith, 1981; Chapman, 1995). The following ratios were calculated: BG/AB, BG/BE, BG/FG, AB/CD and EF/BE in Excel. After preforming PCA on this

dataset with $\log_e$ transformation, six outliers were removed (A.126, B.37, B.12, B.20, FW.6, and FW.5). The control group was within the overlapping area (Figure 8). After its removal, the PCs accounted for 89.336% on Axis 1 (size) for total variance, followed by 6.333% (Axis 2) and 5.152% (Axis 3). Hierarchical clustering with P-values showed that AB/FG - BG/FG, AB/CD – FG/CD and BG/BE – EF/BE ratios were the most correlated pairs (Figure 9).

Comparing the first PCA ([Figure 5](#)) and the second PCA Figure 6), the variance contribution on axis 1 decreased from 95.308 to 89.34% and on the second axis from 1.5 to 6.33% (Table 5). So the PCA performed on ratios has decreased the "size" effect and hence, a better differentiation of morphology of the two shores.
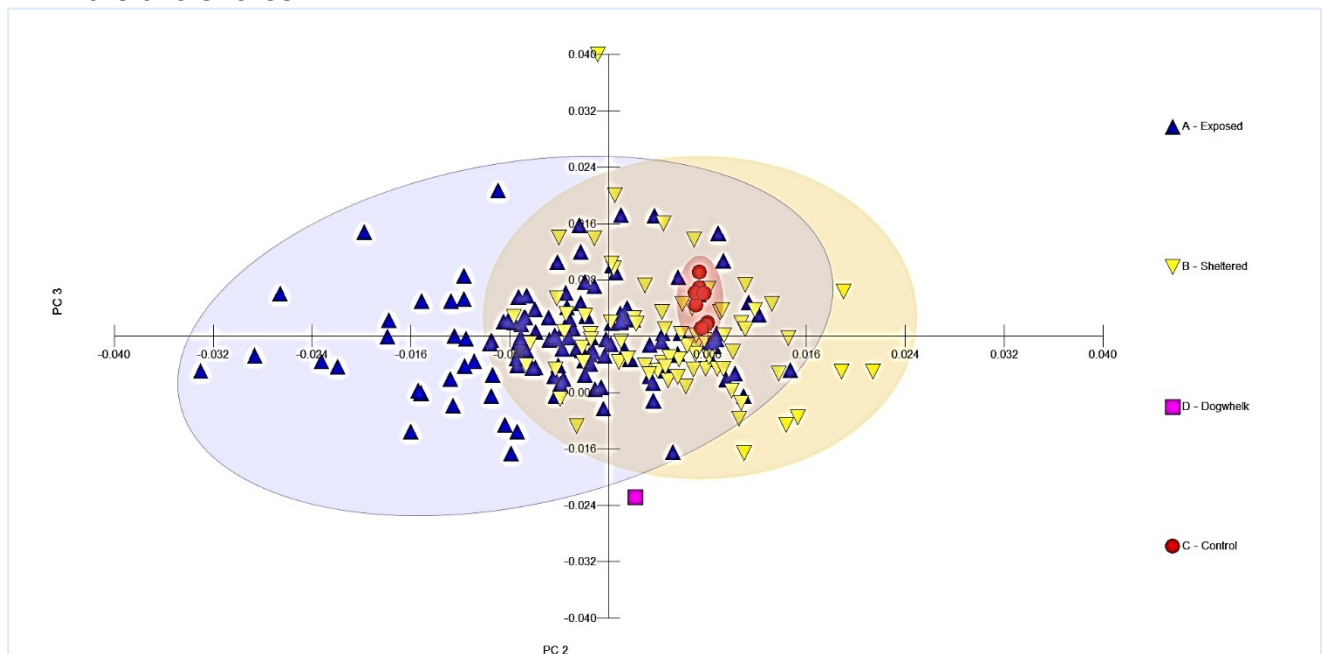

Figure 8. Axis 2 and axis 3 of PCA on ratio data showing a clear separation of the two sites with overlap. Control group (red) are found in the overlap area and the dogwhelk (pink) can be found outside the clusters.

Table 5. Comparing the eigenvalues, and the loading percentages between the $\log_e$ transformed raw data and the ratios on the first three PC axes. Ratios decreased the explained variance (%) on Axis 1.

	Eigenvalues		Percentages		Cum. Percentage	
	$\log_e$	Ratios	$\log_e$	Ratios	$\log_e$	Ratios
Axis 1	1.223	1.456	96.12	89.336	96.12	89.336
Axis 2	0.019	0.103	1.504	6.333	97.624	95.669
Axis 3	0.015	0.07	1.185	4.271	98.81	99.94

Cluster dendrogram with AU/BP values (%)

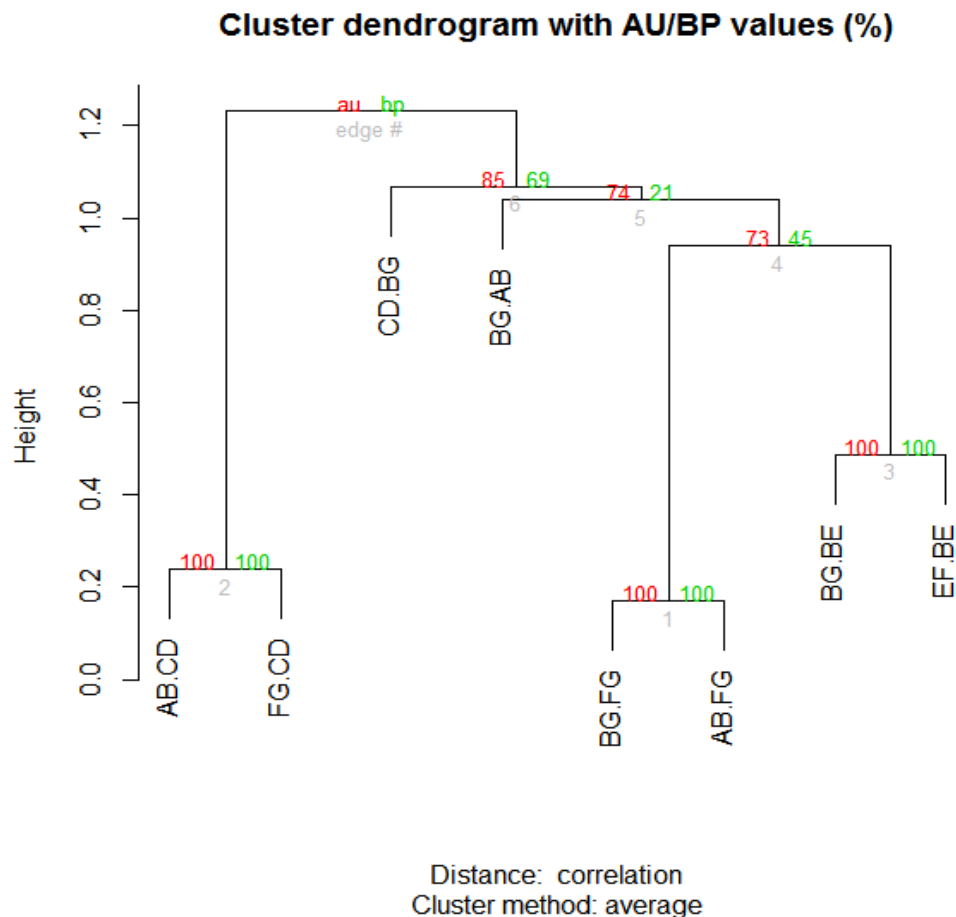Distance: correlation
Cluster method: average

Figure 9. Hierarchical clustering with P-values and bootstrapping interestingly did not cluster the ratio of total length and total width (BG/AB). The ratios of other measurement's to the aperture (FG) width were all significant. This suggest the for the ratio data set, most variance is explained by the ratio of aperture width.

3. Normal PCA on geometric mean transformed data

The following data transformation was developed by Grahame and Mill (1989) to minimise effect of size. It was further developed by Clarke et al. (1999) and incorporated with extended eigenshape method (MacLeod 1999) by Walker and Graham (2011). Calculations were done in Excel (Appendix 3). The apical angle (aa, the pointedness of the shell), assuming that the natural shape of the unconstrained aperture is a circle (Morita, 1991) was also calculated according to Clarke et al. (1999) (Figure 10). The spire expansion rate (W), one parameter from Raup (1961) for simple shell growth modelling, was calculated by the ratio

of the first (CD) and second whorl width. Note that our measurements were not precisely the same as the whorl radiuses in Clarke et al.'s (1999) calculations.
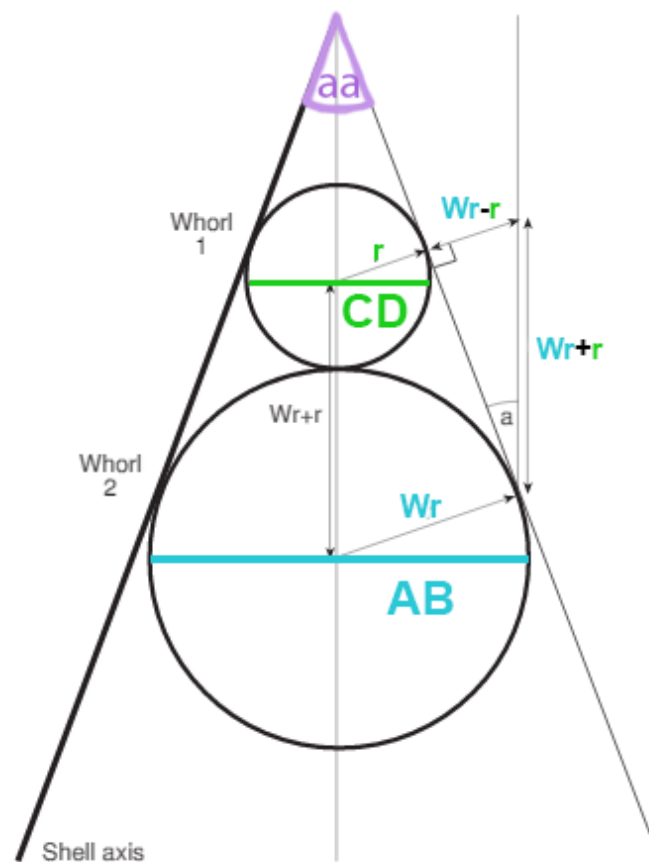
$$W = CD/AB$$

$$aa = 4\sin^{-1}((W - r)/(W + r))$$

Figure 10. Calculations used for the geometric mean (GM) transformed data. Whorl expansion (W) was calculated from the width of the second and first whorl width. Apical angle (aa) describes the shell doming and was calculated by W and the radius of last and second whorl's width, and r is the initial radius generating the curve (illustration adopted from Clarke et al., 1999, Appendix 3).

The PCA on GM transformed measurements did not show a significant change of the explained variance percentages (Axis 1 95.013%, Axis 2 3.667, residuals contribute 1.32%) or eigenvalues compared to the PCA on the normal measurements.

Table 6. PCA results for GM data, showing a combination of positive and negative loadings. Significant variable loadings are shown in bold (<± 0.1).

PCA variable loadings	Axis 1	Axis 2	Axis 3	Axis 4	Axis 5	Axis 6
W	**0.114**	**0.843**	**0.225**	-0.328	-0.235	-0.25
Aa	**0.966**	0.028	**-0.107**	**0.147**	**0.13**	**0.126**
BGt	-0.091	**0.204**	**0.103**	-0.09	**-0.109**	**0.959**
FGt	**-0.1**	0.194	0.141	-0.145	**0.954**	0.029
Eft	**-0.162**	**0.387**	**-0.862**	**0.274**	0.072	0.029
BEt	-0.095	**0.243**	**0.406**	**0.876**	0.014	-0.02
Eigenvalues	1.37	0.053	0.011	0.006	0.002	0
Percentage	95.013	3.667	0.761	0.417	0.11	0.031
Cum. Percentage	95.013	98.68	99.441	99.859	99.969	100

As the GM measurements did not show linear relationship, NMDS was used which showed clear separation between the two sites (Figure 11). Clustering showed that the variables are highly correlated, however W and aa are on a separate node (Figure 12) and a regression in Excel showed a decreasing linear relationship between them (Figure 13).
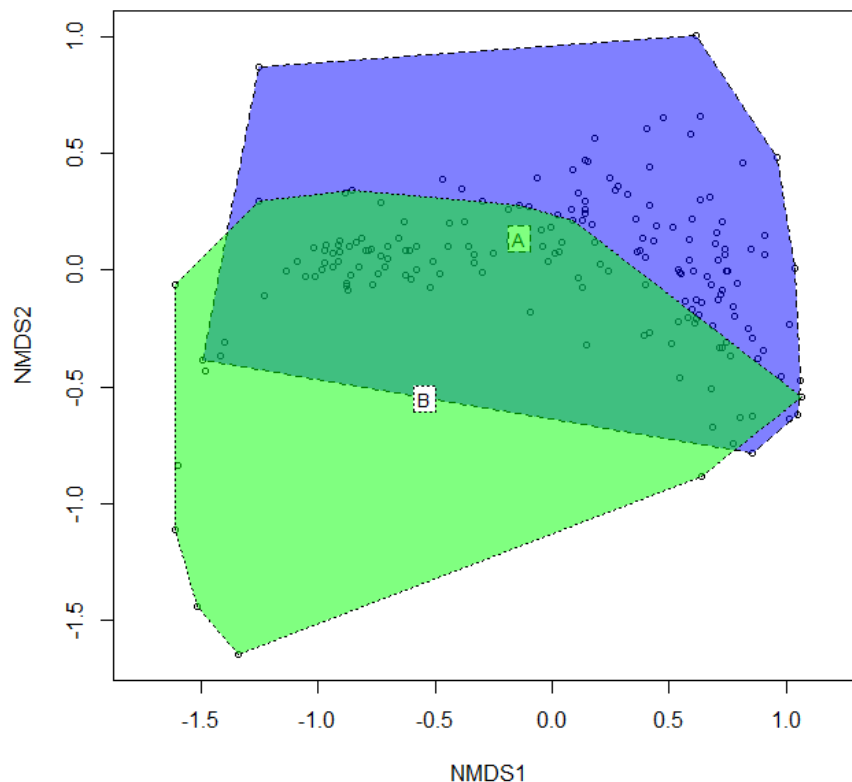

Figure 11. NMDS using the "vegan" package (Oksanen et al., 2013) on GM transformed data set showing clear separation of the two sites with considerable overlap. Control group did not overlap and was removed. The PCA of this data set showed complete overlap. NMDS led to a better presentation because it does not assume linear relationship between variables.
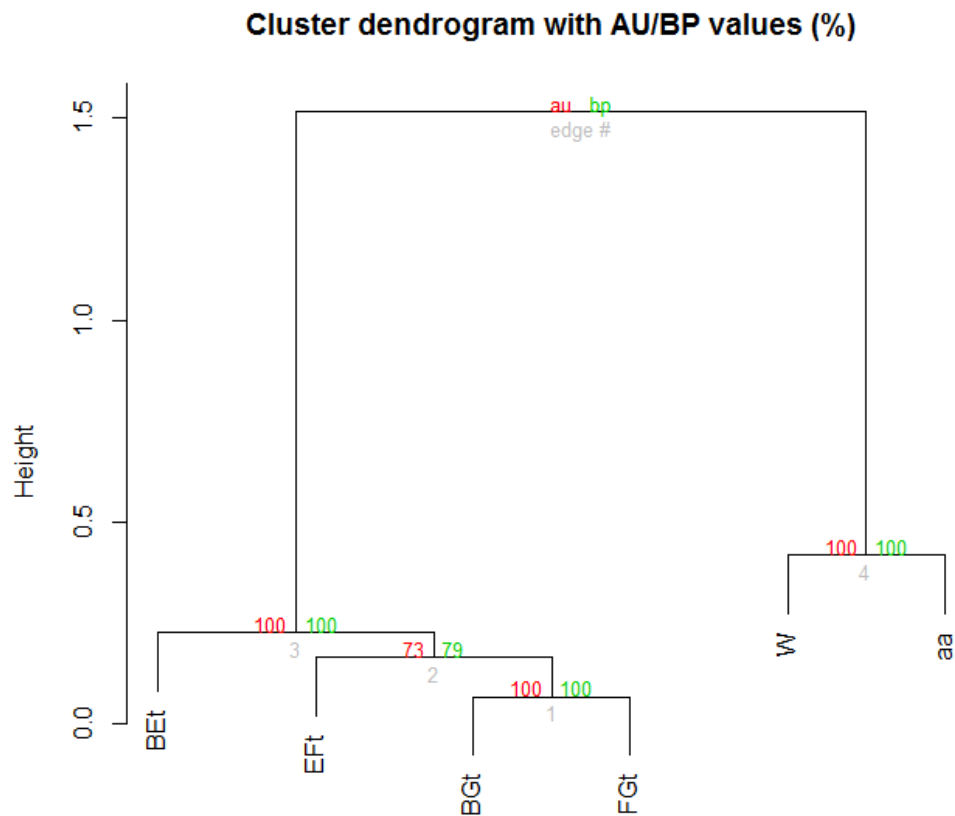
Figure 12. Hierarchical clustering with P-values and bootstrapping (Suzuki and (Shomodaira, 2006) showed that all variables are significant and W and aa form separate node.
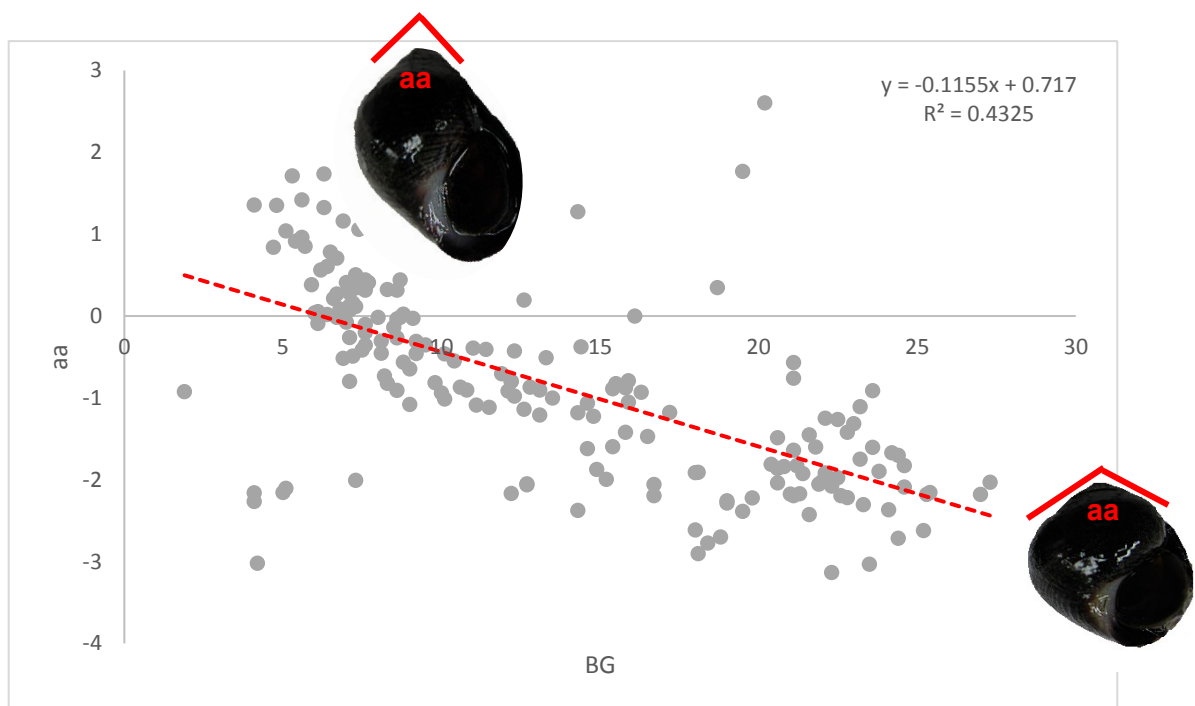

Figure 13. The apical angle is decreases with shell size (total length, BG), which is common in periwinkles (Reid, 1996; Clarke et al., 1999). This leads to a more rounded top of the shell.

4. Explaining PCA axes

With Bayesian PCA ("bPCA" package; Nounou et al., 2002; Li and Tao, 2012), the range of posterior eigenvalue distribution (Table 7) and explained variance was calculated (Table 8). This revealed patterns of variable contribution to different PC axes (Table 9). By combining the information from Bayesian PCA, variable contribution and squared cosine ($\cos^2$, it indicates the contribution of a component to the squared distance of the sample, Abdi and William, 2010), PCA axes can be explained fully (Figure 14). The steps and packages used for these steps are explained in Figure 4. The output for square cosine of different data sets is in the Appendix 4-10 (graphs are summaries of the output). Axes are referred to as PC1, PC2 etc. For variable contribution visualisation at the two sites on PC1, PC2 and PC3 axes see Appendix 11-13.

Table 7. With Bayesian PCA, the distribution of explained variance on different PC axes was investigated. As the hierarchical clustering proved, PC1 is explained by the size of shells. The different percentages of PC2 shows how the different data sets' outputs represent shape contribution. For example, both **log$_e$ and GM** transformed data shows that on exposed shores, the variance explained by PC2 is larger than on sheltered shores. Ratios show a very different pattern – PC2 is explained by 1.402-1.759% on exposed shores but on sheltered shores this percentages is 14.918-18.994%. It can be concluded that the different shell shapes are more expressed on sheltered PC2 axis than on the other data set's PC2.
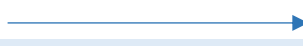
Explained variance (%)

	ln			Ratio			GMt		
Quartile	0.025	0.5	0.975	0.025	0.5	0.975	0.025	0.5	0.975
Exposed		Range							
PC1	91.100	91.910	92.730	95.980	96.330	96.680	91.720	92.470	93.160
PC2	5.291	5.903	6.654	1.402	1.558	1.759	4.485	5.018	5.618
PC3	0.987	1.098	1.228	0.938	1.049	1.180	1.310	1.457	1.627
PC4	0.716	0.807	0.889	0.561	0.629	0.707	0.693	0.773	0.874
Sheltered									
PC1	93.550	94.320	94.960	69.470	72.240	74.810	96.200	96.690	97.120
PC2	2.221	2.551	2.929	14.918	16.825	18.994	2.280	2.671	3.092
PC3	1.631	1.847	2.143	5.167	5.904	6.732	0.287	0.333	0.387
PC4	0.806	0.924	1.084	3.100	3.490	3.999	0.179	0.207	0.240
Both									
PC1	88.330	89.280	90.260	81.690	82.860	83.930	93.720	94.230	94.720
PC2	5.288	5.900	6.564	7.580	8.227	8.940	4.158	4.576	5.044
PC3	2.735	3.020	3.399	4.379	4.720	5.166	0.605	0.665	0.727
PC4	0.788	0.883	0.986	3.092	3.362	3.652	0.332	0.366	0.403

Table 8. Eigenvalues represent the 'strength' of each PC loading. With Bayesian PCA the range of eigenvalues between first, middle and last quartile shows how PC loadings are affected by eigenvalues. For example, both **log$_e$ and GM** data, PC1 values are always larger than PC2 ones. For **ratio**, interestingly on exposed shore, the range is the widest 0.95) and the first quartile on PC2 is larger than on PC2. For GM data, the eigenvalues double on sheltered shores and the range on PC1 (0.354) is the second largest on the data set. This gives an insight how PC loadings and therefore, variable contributions are calculated for PCA.

	ln			Ratio			GMt		
Quartile	0.025	0.5	0.975	0.025	0.5	0.975	0.025	0.5	0.975
Exposed								Range	
PC1	0.851	0.932	1.018	0.025	0.500	0.975	0.793	0.868	0.947
PC2	0.055	0.060	0.065	0.399	0.433	0.468	0.044	0.047	0.051
PC3	0.010	0.011	0.012	0.261	0.282	0.307	0.013	0.014	0.015
PC4	0.008	0.008	0.009	0.187	0.201	0.218	0.007	0.007	0.008
Sheltered									
PC1	0.992	1.114	1.237	0.512	0.583	0.641	1.404	1.566	1.758
PC2	0.027	0.030	0.033	0.120	0.134	0.149	0.039	0.043	0.048
PC3	0.020	0.022	0.024	0.042	0.047	0.052	0.005	0.005	0.006
PC4	0.010	0.011	0.012	0.025	0.028	0.031	0.003	0.003	0.004
Both									
PC1	1.000	1.097	1.193	1.381	1.477	1.583	1.450	1.554	1.676
PC2	0.067	0.072	0.079	0.224	0.241	0.257	0.070	0.076	0.081
PC3	0.035	0.037	0.040	0.081	0.087	0.093	0.010	0.011	0.012
PC4	0.010	0.011	0.012	0.060	0.064	0.068	0.006	0.006	0.006

Table 9. Variable contributions to different PC axes. For the **log$_e$ and GM** transformed data set, the first axis is explained by multiple variables (within 2% difference). For ratios, axis 1 is explained by one variable, the next variable is 5% less. The first and third data set shows the same pattern of variable contribution on exposed and sheltered shores. These variables are in the same order as the hierarchical clustering (Fig 9) identified them to be correlated. The ratio data set show a different pattern, it is clear that different variables contribute to the variance on the two different sites. This helps understanding how the PCA axes are produced.

|	Exposed				Sheltered				Both			
	PC1	PC2	PC3	PC4	PC1	PC2	PC3	PC4	PC1	PC2	PC3	PC4
ln BE	14.91	55.31	28.38	0.88	15.95	73.92	0.43	5.68	16.03	52.91	29.27	0.18
ln EF	15.03	43.96	40.94	0.02	16.01	8.15	70.05	0.35	16.08	45.50	33.90	4.19
ln FG	17.38	0.11	4.60	37.56	16.89	2.26	15.05	22.58	17.15	0.33	5.87	2.62
ln CD	17.18	0.35	11.26	58.52	16.49	15.63	9.04	57.91	16.80	0.00	23.48	14.98
ln AB	17.60	0.27	10.07	1.47	17.18	0.05	5.29	12.66	17.25	0.00	6.05	0.70
ln BG	17.89	0.00	4.74	1.55	17.47	0.00	0.14	0.82	16.69	1.26	1.44	77.33
AB/CD	22.629	12.626	9.609	9.028	29.17	3.72	9.10	4.57	26.926	10.446	12.491	0.610
AB/FG	27.525	2.305	21.261	0.003	18.06	12.62	1.21	30.29	27.348	8.810	9.986	6.583
BG/AB	3.426	3.430	3.527	68.010	5.65	26.73	3.29	33.11	5.552	1.600	5.585	62.267
BG/BE	7.143	28.498	11.813	0.522	6.23	0.14	49.75	0.49	1.088	29.434	20.742	0.496
BG/FG	22.177	0.266	15.740	19.988	5.79	48.74	0.05	0.87	17.447	14.584	22.556	4.224
CD/BG	15.345	22.326	17.583	1.754	23.17	0.00	6.17	30.64	20.891	7.935	6.620	22.504
EF/BE	1.755	30.549	20.468	0.696	11.94	8.05	30.44	0.03	0.747	27.191	22.018	3.317
W	1.605	80.571	1.373	0.983	11.934	60.520	1.682	3.554	3.456	81.385	0.585	1.577
aa	22.161	9.404	0.132	2.185	19.710	9.286	0.249	0.042	20.673	6.928	0.269	1.383
BGt	22.060	3.403	0.233	15.259	20.187	3.471	0.339	1.654	20.997	2.136	0.203	9.045
FGt	21.948	1.036	0.171	18.940	17.507	2.810	1.428	58.429	20.332	1.548	0.282	33.294
EFt	17.194	0.938	38.109	42.418	16.082	3.929	61.766	9.591	17.835	2.915	38.674	37.520
BEt	15.031	4.647	59.983	20.216	14.580	19.983	34.535	26.729	16.708	5.088	59.988	17.181
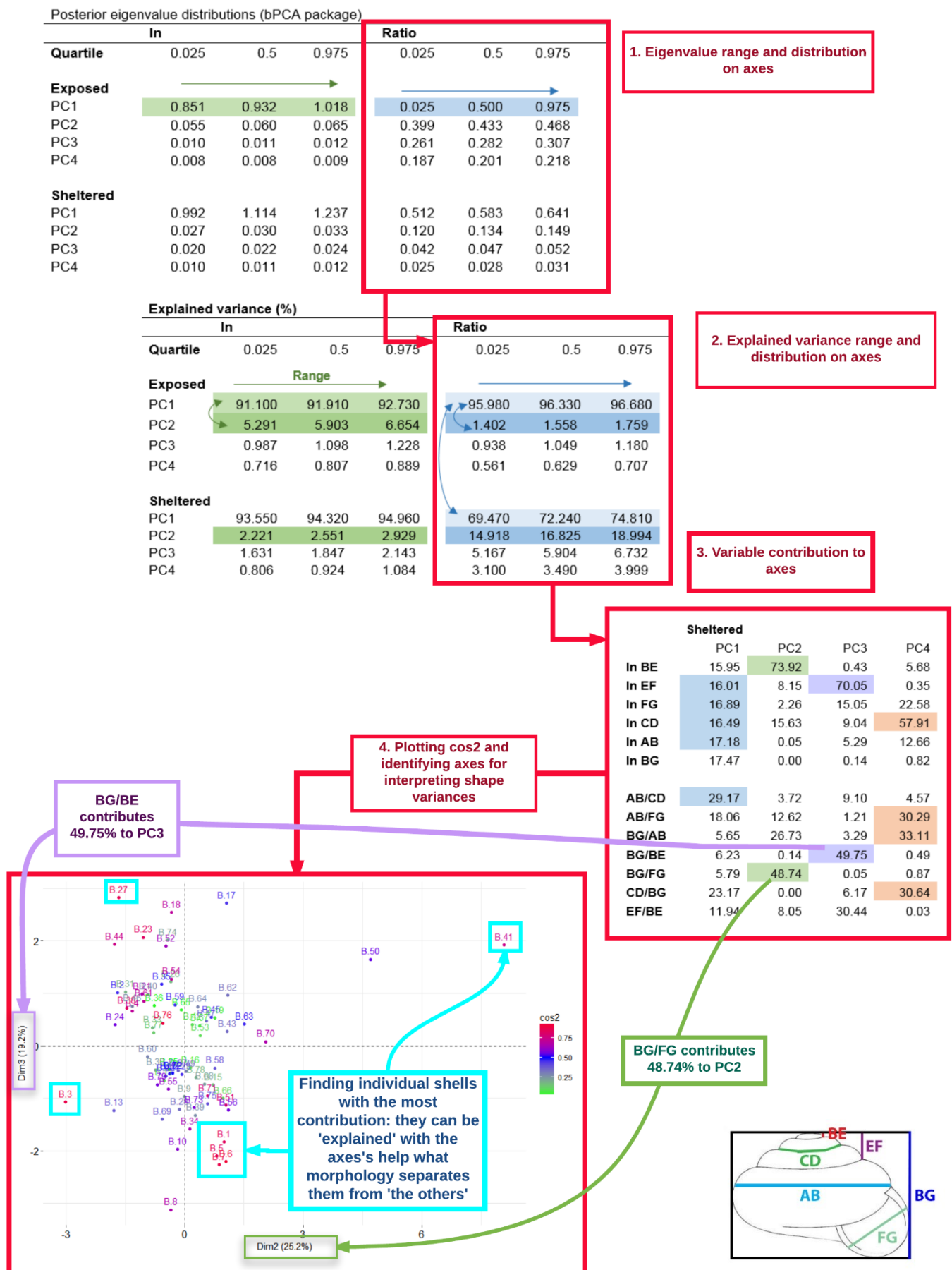
Figure 14. Flowchart of how the PCA axes can be explained by understanding the posterior eigenvalue, explained variance distribution, then the variable contribution to different axes. This example is for **sheltered ratio data**. After plotting cos², each shell's contribution can be explained by referring back to variable contribution to the axes. For example, B.41 shell has a high contribution to PC2 and PC3 (colour red), it shows high BG/FG (4.3) ratio, but it has a lower BG/BE ratio (3.2) than B.27 shell (6.9) (see Appendix 4). By plotting each data set separately and explaining the PC axes in this way, most samples can be explained this way.

DISCUSSION

The aim of this paper was to investigate different shell shapes on exposed and sheltered shores. A combined multivariate approach was suggested for finding underlying shape differences. The most variance was caused by the shells' sizes, exposed shells were smaller than the ones collected at the sheltered site. PCA is the most widely used multivariate analysis, however in most cases, the contribution of each variable and consequently each individual is not examined (Smith, 1981; Johannesson et al., 1993; Chapman, 1997). PC loadings on $\log_e$ data was similar to result reported by Johannesson et al.'s (1993) who could not detect a clear pattern of PC2s of their 13 quantitative shell characters. By investigating the posterior distribution of eigenvalues and their effect of the explained variance of different PC axes, and the contribution of each variable can be investigated.

Bayesian PCA showed that for the $\log_e$ transformed raw data, three or four variables contributed to PC1 associated with length, width and aperture width. For ratios, one measurement was significantly more than the others (AB/FG on exposed and AB/CD on sheltered). For GM transformed data, interestingly W contributed the most to PC2 as opposed to Walker and Grahame (2011), where W was mostly contributing to PC1. Clarke et al. (1999) and Walker and Grahame (2011) found that apical angle (aa) decreases with shell size which was the same (Figure 13) for this study.

The PCA did not entirely separate the two group as (1) *Littorina* move across the shore (Gendron, 1977; Janson, 1983; Rolan-Alvarez et al., 1997; Erlandsson et al., 1998), (2) their morphology can be affected by sex and reproductive stage (Takada, 2003; Pardo and Johnson, 2004) and (3) they

hybridize (Boulding, 1990; Cruz et al., 2001). Habitat selection (Erlandsson et al., 1998; Jones and Boulding, 1999), different rock surfaces, habitat complexity (Rolan-Alvarez et al., 1997; Pardo and Johnson, 2003; Queiroga et al., 2011), salinity are also variables to consider in *Littorina* distribution (Smith, 1981; Johannesson, 1986). Growth rate and snail density also affects shell shape (Kemp and Bertness, 1984; Kitching and Lockwood, 1974; Trussell et al., 2006) and therefore the resource availability should also be considered.

In this study, neither the age nor the sex (nor reproductive stage) of the individual rough periwinkles was determined which would have added valuable information to our data's interpretation. Chapman (1995) found that the size and shape mean values differed between high shore sites within a 50 meter interval. It would have been useful to have the transects further apart (instead of 54 meter).

The evolution of shell ecotypes is still debatable as they are genetically similar despite their morphology (Johannesson et al., 1993; Trussell, 2002; Wildling et al., 2001). It could be a target of selection (Scheiner, 1993; Rolan-Alvarez et al., 2015; Conde-Padin et al., 2009) or a by-product (Via, 1994; Cruz et al., 2004). Therefore, if all of the above variables and genetic analysis would be collected in further studies, with precise multivariate modelling, we could gain a full understanding of *Littorina* distribution.

APPENDIX

> **Appendix 1.** Describing the data sets by mean ± SE. Sample sizes after outlier removal with the help of scatterplot visualisation.

n=204	Mean ± SE	n=188	Mean ± SE	n=202	Mean ± SE
ln BE	0.854 ± 0.040	**W**	1.836 ± 0.022	**AB/CD**	1.845 ± 0.022
ln EF	0.836 ± 0.052	**aa**	-0.716 ± 0.086	**AB/FG**	1.280 ± 0.011
ln FG	2.081 ± 0.038	**BGt**	0.773 ± 0.009	**BG/AB**	1.245 ± 0.006
ln CD	1.724 ± 0.039	**FGt**	0.581 ± 0.009	**BG/BE**	5.513 ± 0.084
ln AB	2.309 ± 0.035	**EFt**	0.044 ± 0.016	**BG/FG**	1.579 ± 0.013
ln BG	2.512 ± 0.037	**BEt**	0.052 ± 0.011	**CD/BG**	0.458 ± 0.004
				EF/BE	1.053 ± 0.023

> **Appendix 2.** Correlation matrices for each data set.

	ln BE	ln EF	ln FG	ln CD	ln AB
ln EF	0.877				
ln FG	0.927	0.921			
ln CD	0.907	0.909	0.959		
ln AB	0.926	0.927	0.978	0.965	
ln BG	0.907	0.917	0.945	0.933	0.953

	BG/AB	BG/BE	AB/CD	BG/FG	EF/BE
BG/AB	-0.107				
BG/BE	-0.383	0.023			
AB/CD	0.196	0.122	0.098		
BG/FG	0.133	0.512	-0.118	0.002	
EF/BE	-0.377	0.185	0.299	0.831	-0.071

	W	aa	BGt	FGt	EFt
aa	0.536				
BGt	-0.028	-0.831			
FGt	-0.118	-0.825	0.878		
EFt	-0.090	-0.710	0.719	0.706	
BEt	-0.029	-0.604	0.686	0.665	0.504

> **Appendix 3.** Calculation of GM data set.

The geometric mean (GM) of all measurement is the logarithm of each measurement divided by the number of measurements:

$$GM = log_{10}{}^{-1}(\frac{log_{10}(BE) + log_{10}(EF) + log_{10}(FG) + log_{10}(CD) + log_{10}(AB) + log_{10}(BG)}{6})$$

Then each measurement is transformed in this way (example of BG):

$$BG_t = log_{10}(\frac{BG}{GM})$$

Whorl expansion was the ratio of the first whorl width (CD) and the second whorl width (in this case AB, total width):

$$W = \frac{CD}{AB}$$

Apical angle (aa) was calculated as the unconstrained natural shape of an aperture is suggested to be a circle (Morita, 1991):

$$aa = 4sin^{-1}\frac{(W - r)}{(W + r)}$$

Where r is half of the first whorl width (CD).

Appendix 4. Cos^2 for sheltered ratios data set. Individual shells are organised in a descending order per PC. Examples used in text highlighted.

Column continued…

ID	PC1	PC2	PC3				
B.66	7.069	0.617	0.869	B.69	1.631	0.216	1.699
B.25	6.703	0.107	0.179	B.16	1.540	0.014	0.153
B.31	6.097	1.481	0.911	B.13	1.462	2.101	1.313
B.19	5.840	0.393	0.244	B.8	1.303	0.081	8.451
B.74	5.594	0.124	3.507	B.15	1.216	0.349	0.480
B.50	5.582	14.570	2.339	B.39	1.187	0.047	1.515
B.65	4.749	0.004	0.399	B.9	1.130	0.000	0.805
B.17	4.175	0.737	6.379	B.33	1.060	0.435	0.105
B.41	**3.602**	**43.137**	**3.191**	B.10	0.959	0.023	3.370
B.26	2.901	0.084	1.281	B.52	0.945	0.152	3.116
B.46	2.689	1.158	0.497	B.60	0.862	0.577	0.037
B.11	2.268	0.176	0.374	B.53	0.820	0.103	0.033
B.36	14.710	0.382	0.506	B.24	0.790	2.049	0.139
B.2	1.810	1.894	0.882	B.18	0.787	0.076	5.586
B.62	1.691	0.776	0.799	B.35	0.693	0.220	1.193
				B.70	0.676	2.787	0.005

B.3	0.553	6.027	0.988	B.6	0.158	0.726	4.220
B.67	0.462	0.092	0.126	B.34	0.140	0.013	2.185
B.30	0.417	0.360	0.180	B.44	0.140	2.085	3.227
B.47	0.379	0.199	0.194	B.29	0.139	0.004	0.253
B.63	0.337	1.491	0.150	**B.27**	**0.136**	**1.826**	**6.896**
B.5	0.298	0.438	3.819	B.28	0.114	0.013	1.277
B.21	0.288	0.770	0.839	B.57	0.106	0.016	0.195
B.7	0.275	0.504	4.444	B.4	0.059	1.148	0.377
B.48	0.264	0.160	0.284	B.45	0.045	0.292	0.254
B.58	0.258	0.384	0.153	B.38	0.043	1.414	0.444
B.1	0.245	0.668	2.898	B.40	0.038	0.553	0.833
B.54	0.241	0.075	1.397	B.22	0.028	0.148	0.285
B.42	0.233	0.025	0.143	B.72	0.026	0.063	0.238
B.77	0.222	0.404	0.054	B.59	0.025	0.036	0.530
B.79	0.214	0.310	0.470	B.73	0.024	0.037	1.205
B.64	0.212	0.071	0.480	B.68	0.010	0.165	0.457
B.49	0.206	0.001	0.208	B.71	0.009	0.222	0.787
B.51	0.202	0.719	1.108	B.76	0.009	0.204	0.160
B.61	0.196	0.695	0.624	B.32	0.008	0.095	0.245
B.55	0.185	0.108	0.591	B.75	0.005	0.219	1.047
B.78	0.182	0.054	0.318	B.56	0.003	0.819	1.302
B.43	0.166	0.753	0.064				
B.23	0.160	0.723	3.693				

Appendix 5.* Cos^2 for sheltered log$_e$ data set. Axis 2 BE (73.92%), Axis 3 EF (70.05%).

*Please note that the author is aware that raw data is expected to be reported in the appendix, but to satisfy the word limit without losing valuable information justifies including graphs in the appendix.
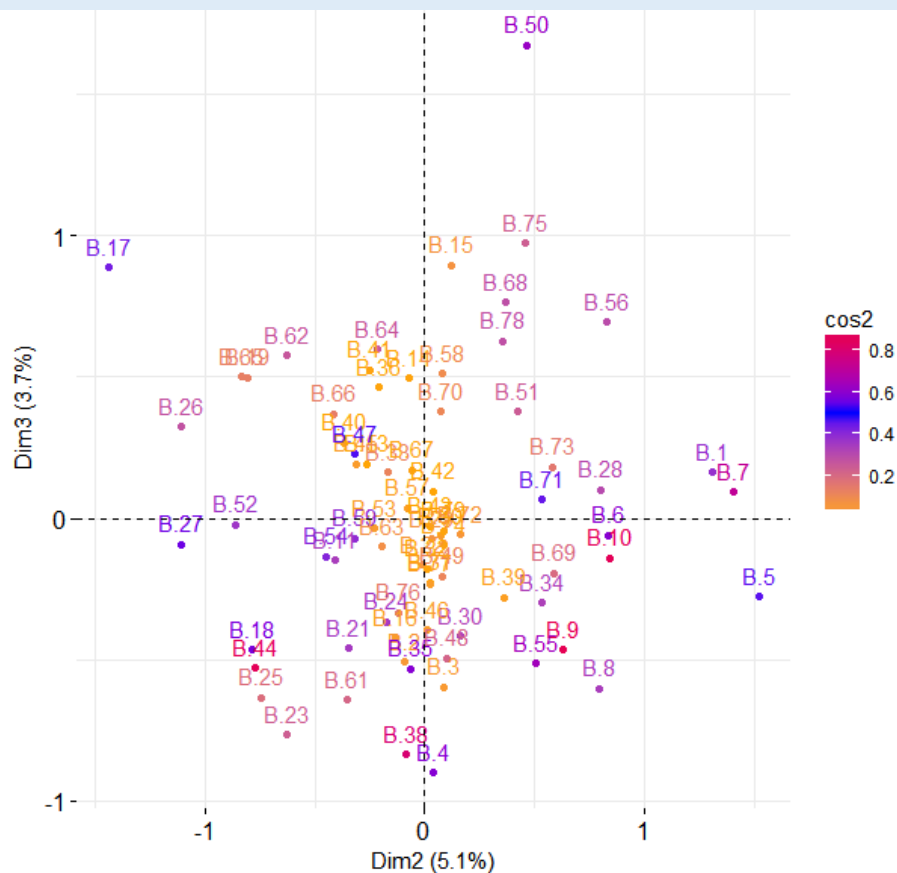
Appendix 6. Cos^2 for sheltered ratios data set. Axis 2 is associated with BG/FG (48.74%) and Axis 3 with BG/BE (49.75%). Percentages indicate variable contribution.
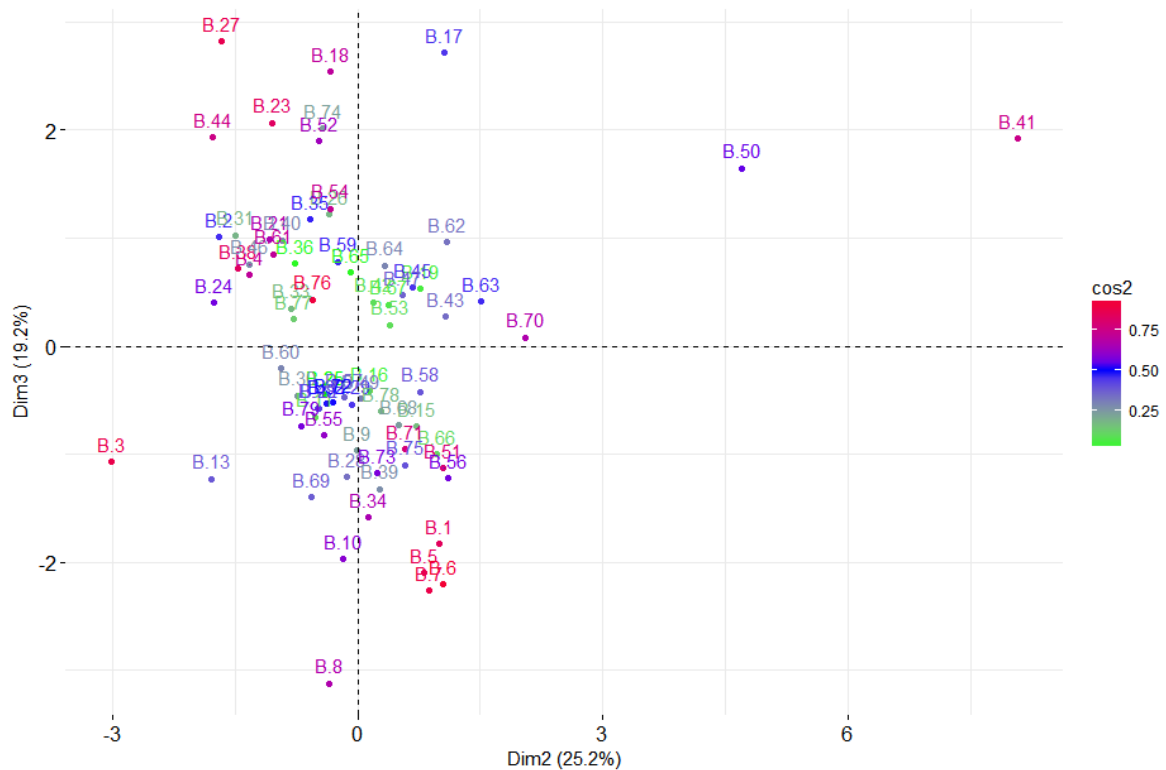

Appendix 7. Cos^2 for sheltered GM data set. Axis 2 associated with W (60.52%), and Axis 3 with EF_t (61.766%). Percentages indicate variable contribution.
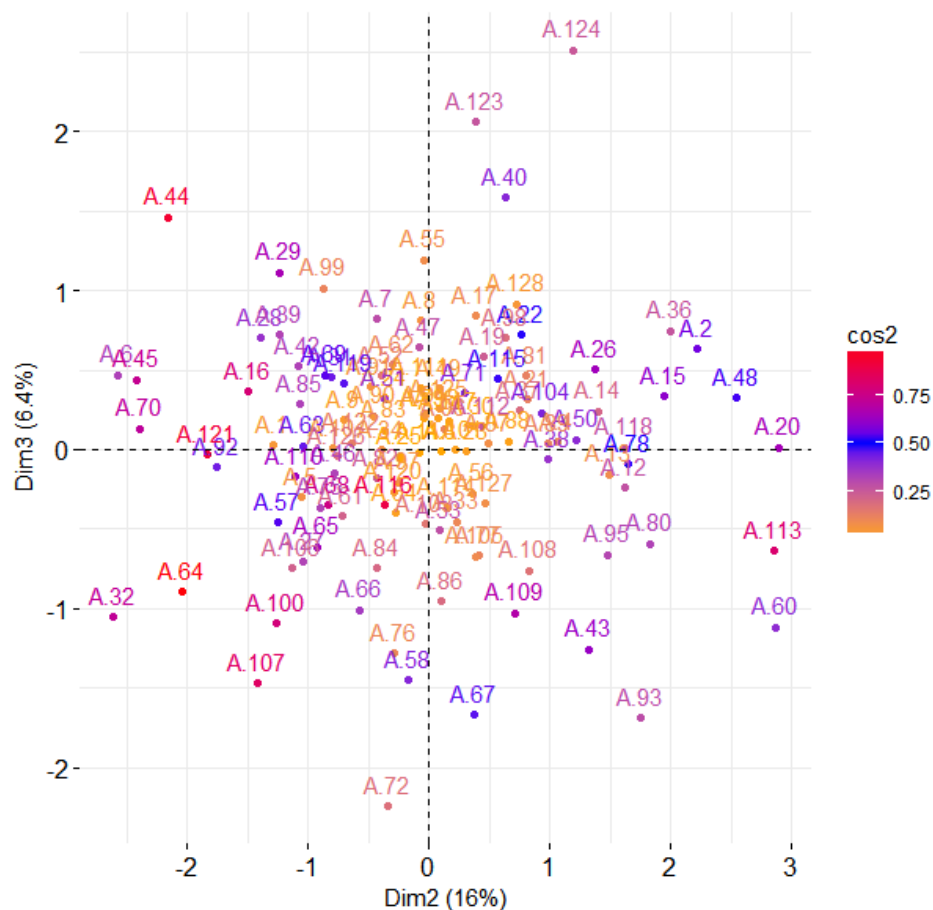
Appendix 8. Cos^2 for exposed log$_e$ data set. Axis 2 associated with BE (55.31%), and Axis 3 with EF (40.94%). Percentages indicate variable contribution.
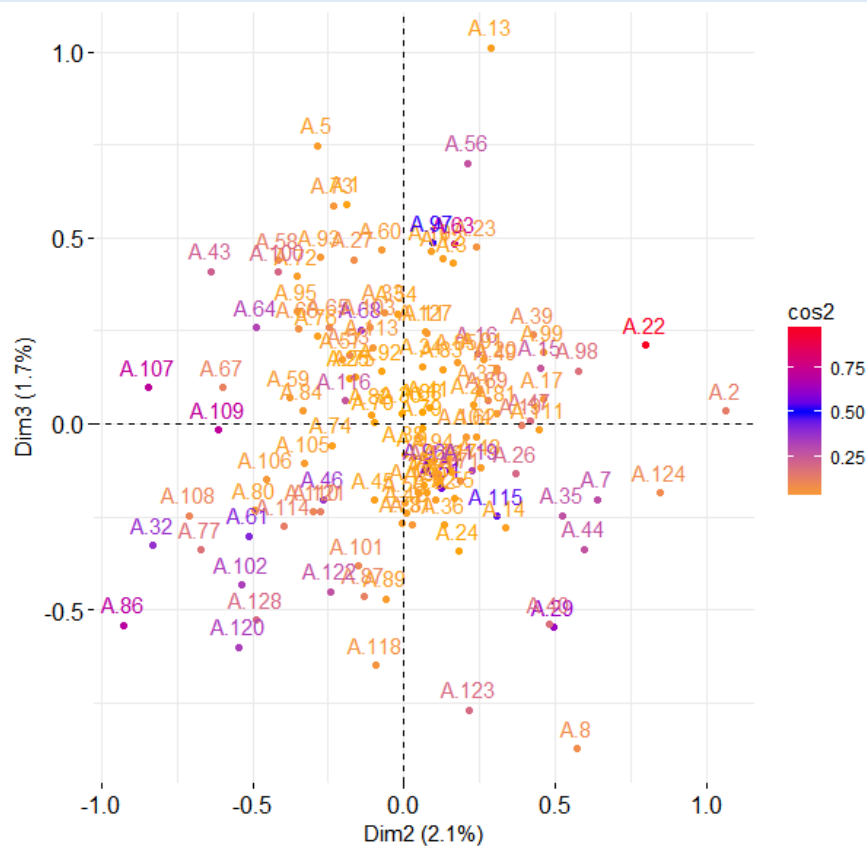

Appendix 9. Cos^2 for exposed ratio. Axis 2 associated with EF/BE (30.549%), and Axis 3 with AB/FG (21.261) and EF/BE (20.468%). Percentages indicate variable contribution.
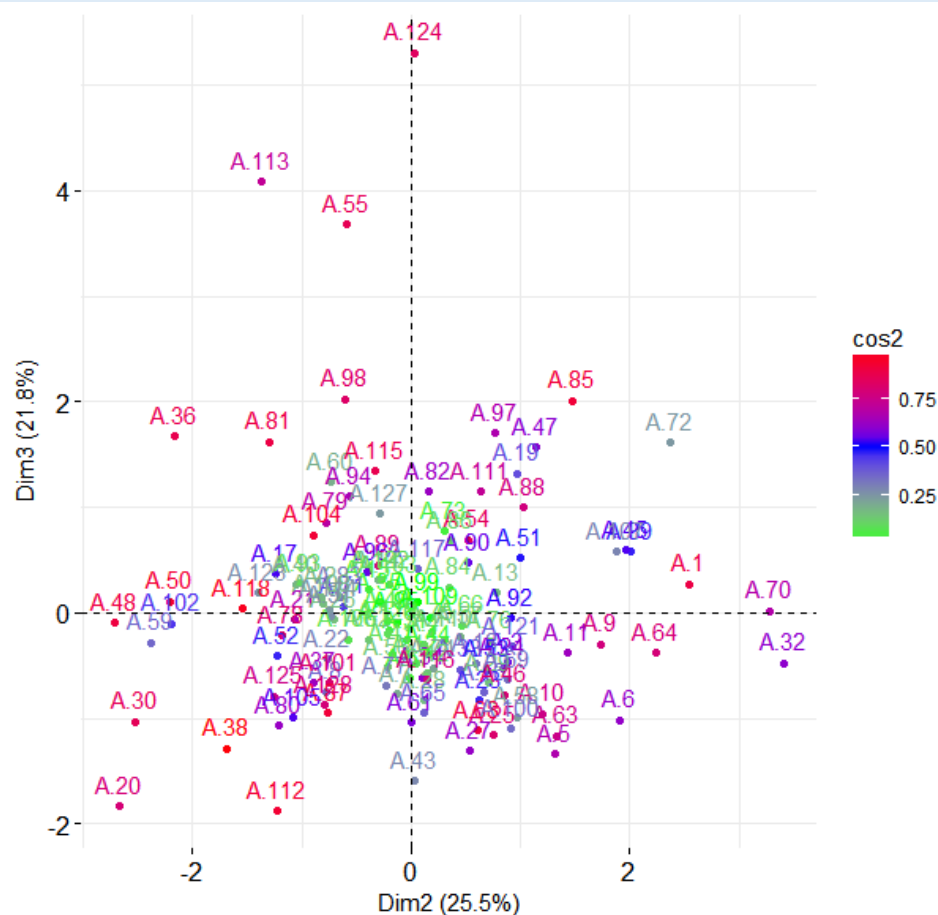
Appendix 10. Cos² for exposed GM. Axis 2 associated with W (80.571%), and Axis 3 with BEt (59.983%). Percentages indicate variable contribution.
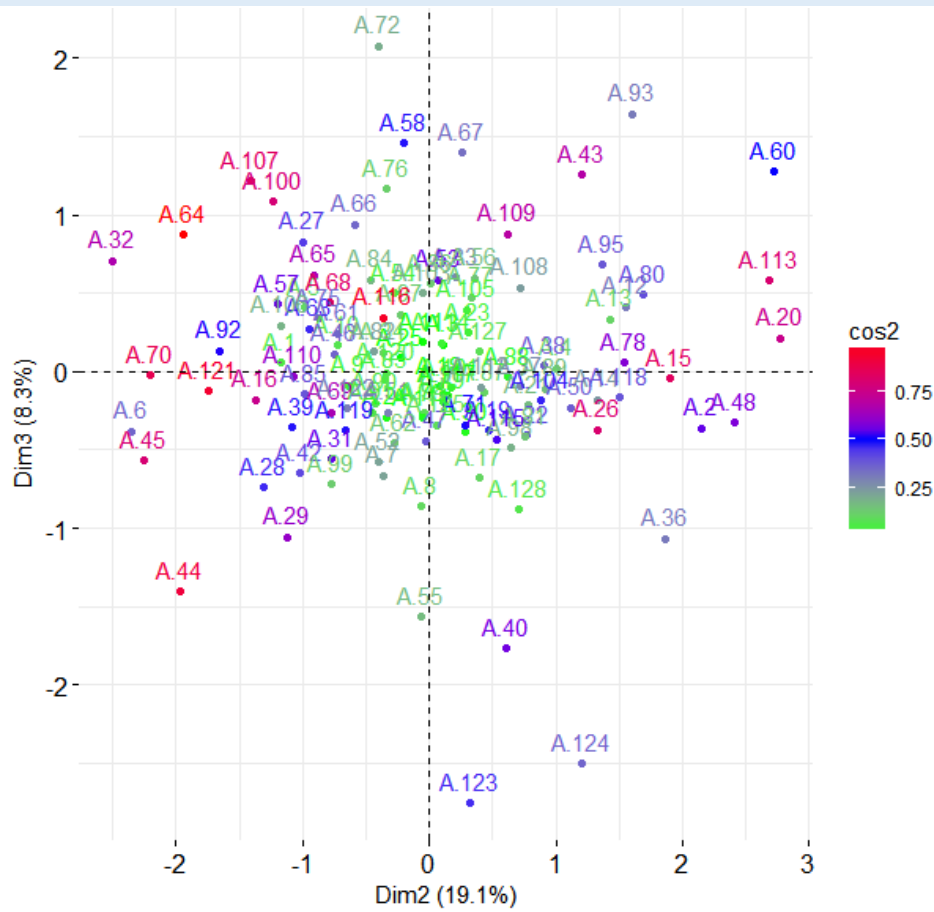
Appendix 11. PCA on $\log_e$ data with varimax rotation comparing the two sites. First graph showing Axis 1 and Axis 2, graph below showing Axis 2 and Axis 3. Contribution of variables are plotted in Euclidian distance matrix, and their colour's intensity indicates the level of contribution. First graph separates shells according to their sizes, while in the second graph, the sheltered site 'sits' in the exposed shell morphology (mostly explained by EF and BE).
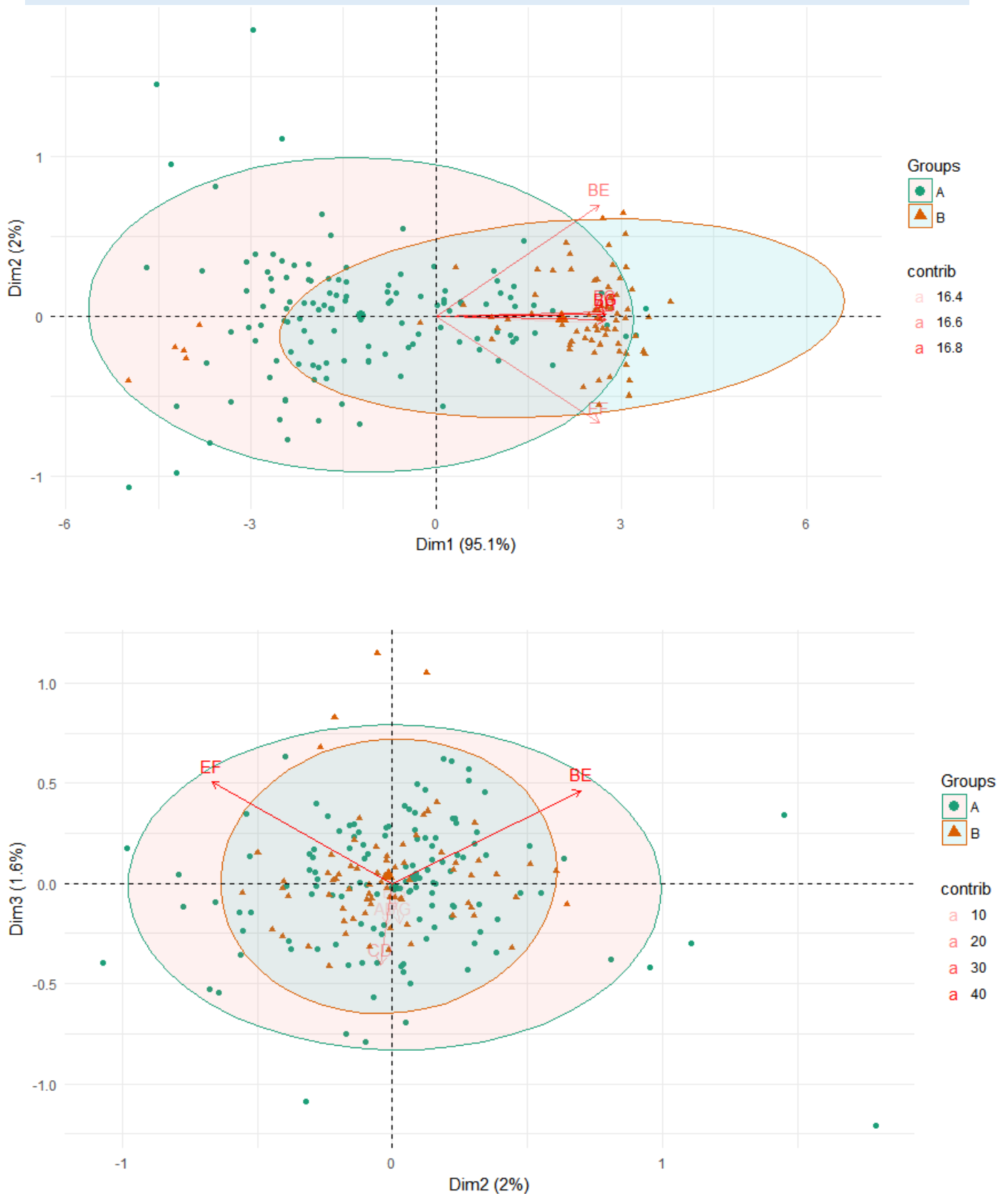
Appendix 12. PCA on ratios with varimax rotation comparing the two sites. First graph showing Axis 1 (27. 348% of AB/FG and 26.926% of AB/CD) and Axis 2 (29.434% of BG/BE and 27.191% of EF/BE), graph below showing Axis 2 and Axis 3 (20.742% of BG/BE, 22.556% of BG/FG, and 22.018% of EF/BE). Percentages indicate variable contribution. Second graph resembles Appendix 11.
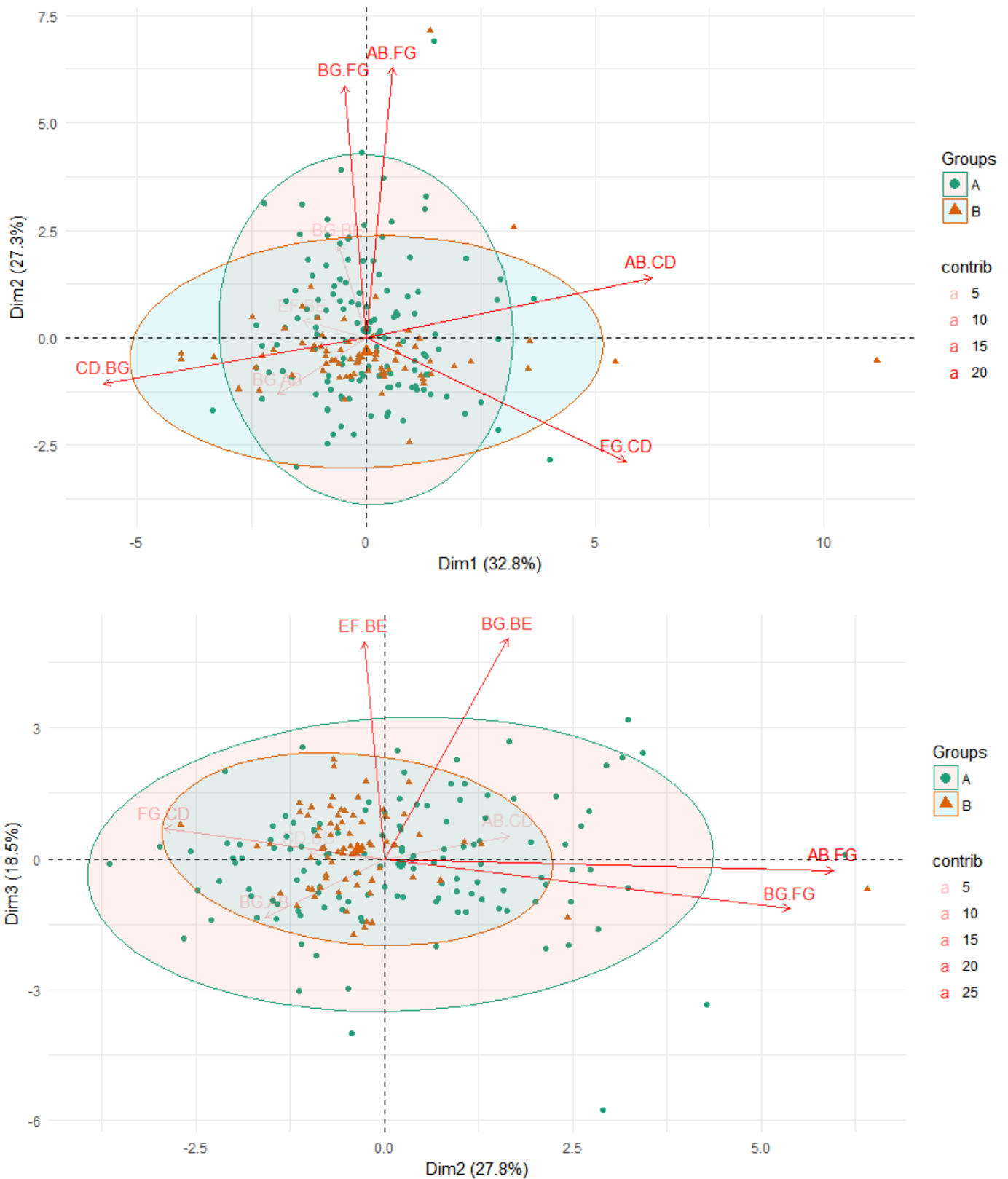
Appendix 13. PCA on GM data with varimax rotation comparing the two sites. First graph showing Axis 1 (20.673% of aa, 20.997% of BG_t, an 20.332% of FG_t) and Axis 2 (81.385% of W), graph below showing Axis 2 and Axis 3 (59.988% of BE_t). Percentages indicate variable contribution.
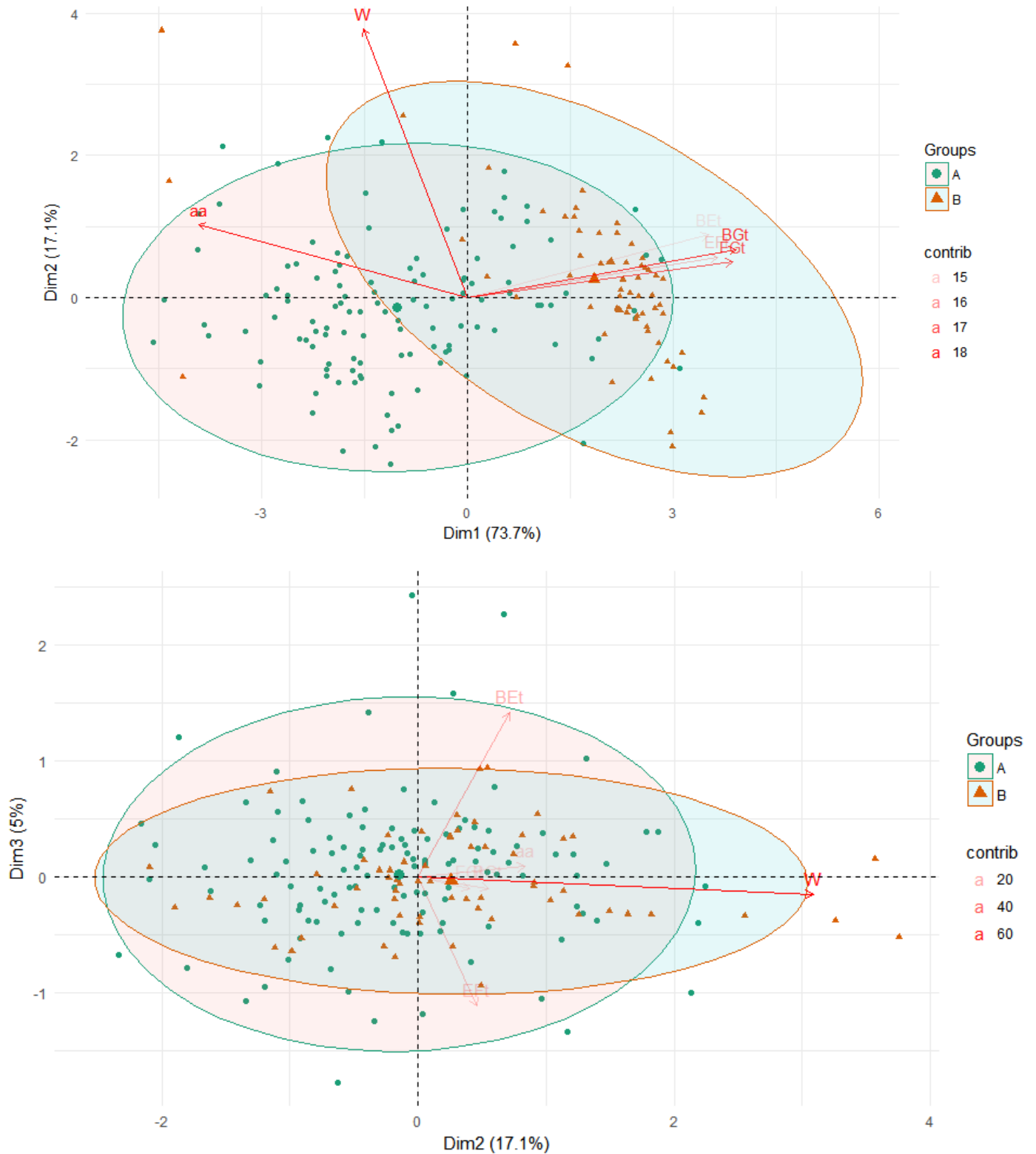
REFERENCES

Abdi, H. and Williams, L.J., 2010. Principal component analysis. *Wiley interdisciplinary reviews: computational statistics, Vol 2(4),* pp.433-459

Agrawal, A.A., 2001. Phenotypic plasticity in the interactions and evolution of species. *Science, Vol 294(5541),* pp.321-326

Bakshi, B.R., 1998. Multiscale PCA with application to multivariate statistical process monitoring. *AIChE journal, Vol 44(7),* pp.1596-1610

Béguinot, J., 2014. Covarying shell growth parameters and the regulation of shell shape in marine bivalves: a case study on Tellinoidea. *Journal of Marine Biology, Vol 2014*

Bishop, C.M., 1999. Bayesian pea. In: *Proceedings of the 1998 conference on Advances in neural information processing systems II*, pp.382-388

Carballo, M., García, C. and Rolán-Alvarez, E., 2001. Heritability of shell traits in wild *Littorina saxatilis* populations: results across a hybrid zone. *Journal of Shellfish Research, Vol 20(1),* pp.415-422

Chapman, M.G., 1995. Spatial patterns of shell shape of three species of co-existing littorinid snails in New South Wales, Australia. *Journal of Molluscan studies, Vol 61(2),* pp.141-162

Clarke, R.K., Grahame, J. and Mill, P.J., 1999. Variation and constraint in the shells of two sibling species of intertidal rough periwinkles (Gastropoda: *Littorina* spp.). *Journal of Zoology, Vol 247(2),* pp.145-154

Clarke, R.K., Grahame, J. and Mill, P.J., 1999. Variation and constraint in the shells of two sibling species of intertidal rough periwinkles (Gastropoda: *Littorina* spp.). *Journal of Zoology, Vol 247(2),* pp.145-154

Conde-Padín, P., Caballero, A. and Rolán-Alvarez, E., 2009. Relative role of genetic determination and plastic response during ontogeny for shell-shape traits subjected to diversifying selection. *Evolution, Vol 63(5),* pp.1356-1363

Conde-Padín, P., Grahame, J.W. and Rolán-Alvarez, E., 2007. Detecting shape differences in species of the *Littorina saxatilis* complex by morphometric analysis. *Journal of Molluscan Studies, Vol 73(2),* pp.147-154

Cruz, R., Carballo, M., Conde-Padín, P. and Rolán-Alvarez, E., 2004. Testing alternative models for sexual isolation in natural populations *of Littorina saxatilis*: indirect support for by-product ecological speciation? *Journal of evolutionary biology, Vol 17(2),* pp.288-293

Cruz, R., Rolán-Álvarez, E. and García, C., 2001. Sexual selection on phenotypic traits in a hybrid zone of *Littorina saxatilis* (Olivi). *Journal of Evolutionary Biology, Vol 14(5),* pp.773-785

De Wolf, H., Backeljau, T., Medeiros, R. and Verhagen, R., 1997. Microgeographical shell variation *in Littorina striata*, a planktonic developing periwinkle. *Marine Biology, Vol 129(2),* pp.331-342

Erlandsson, J., Rolán-Alvarez, E. and Johannesson, K., 1998. Migratory differences between ecotypes of the snail *Littorina saxatilis* on Galician rocky shores. *Evolutionary Ecology, 12(8),* pp.913-924

Etter, R.J., 1988. Asymmetrical developmental plasticity in an intertidal snail. *Evolution,* pp.322-334

Fraley, C. and Raftery, A.E., 1998. How many clusters? Which clustering method? Answers via model-based cluster analysis. *The Computer Journal, Vol 41(8),* pp.578-588

Gendron, R.P., 1977. Habitat selection and migratory behaviour of the intertidal gastropod *Littorina littorea* (L.). The Journal of Animal Ecology, pp.79-92.

Grahame, J. and Mill, P.J., 1986. Relative size of the foot of two species of *Littorina* on a rocky shore in Wales. *Journal of Zoology, Vol 208(2),* pp.229-236

Grahame, J. and Mill, P.J., 1989. Shell shape variation in *Littorina saxatilis* and *L. arcana*: a case of character displacement? *Journal of the Marine Biological Association of the United Kingdom, Vol 69(4),* pp.837-855

Heller, J., 1976. The effects of exposure and predation on the shell of two British winkles. *Journal of Zoology, Vol 179(2),* pp.201-213

Helmuth, B.S. and Hofmann, G.E., 2001. Microhabitats, thermal heterogeneity, and patterns of physiological stress in the rocky intertidal zone. *The Biological Bulletin, Vol 201(3),* pp.374-384

Hollander, J., Adams, D.C. and Johannesson, K., 2006. Evolution of adaptation through allometric shifts in a marine snail. *Evolution, Vol 60(12),* pp.2490-2497

Hull, S.L., Grahame, J. and Mill, P.J., 1996. Morphological divergence and evidence for reproductive isolation in *Littorina saxatilis* (Olivi) in northeast England. *Journal of Molluscan Studies, Vol 62(1),* pp.89-99

Janson, K. and Sundberg, P., 1983. Multivariate morphometric analysis of two varieties of *Littorina saxatilis* from the Swedish west coast. *Marine Biology, Vol 74(1),* pp.49-53

Janson, K., 1982. Genetic and environmental effects on the growth rate of *Littorina saxatilis. Marine Biology, Vol 69(1),* pp.73-78

Janson, K., 1983. Selection and migration in two distinct phenotypes of *Littorina saxatilis* in Sweden. *Oecologia, Vol 59(1),* pp.58-61

Johannesson, B., 1986. Shell morphology of *Littorina saxatilis* Olivi: the relative importance of physical factors and predation. *Journal of Experimental Marine Biology and Ecology, Vol 102(2-3),* pp.183-195

Johannesson, K., 2003. Evolution in Littorina: ecology matters*. Journal of Sea Research, Vol 49(2),* pp.107-117

Johannesson, K., Johannesson, B. and Rolan-Alvarez, E., 1993. Morphological differentiation and genetic cohesiveness over a microenvironmental gradient in the marine snail *Littorina saxatilis. Evolution,* pp.1770-1787

Johannesson, K., Rolan-Alvarez, E. and Ekendahl, A., 1995. Incipient reproductive isolation between two sympatric morphs of the intertidal snail *Littorina saxatilis. Evolution,* pp.1180-1190

Jones, K.M.M. and Boulding, E.G., 1999. State-dependent habitat selection by an intertidal snail: the costs of selecting a physically stressful microhabitat. *Journal of Experimental Marine Biology and Ecology, Vol 242(2),* pp.149-177

Kemp, P. and Bertness, M.D., 1984. Snail shape and growth rates: evidence for plastic shell allometry in *Littorina littorea. Proceedings of the National Academy of Sciences, Vol 81(3),* pp.811-813

Kenkel, N.C. and Orlóci, L., 1986. Applying metric and nonmetric multidimensional scaling to ecological studies: some new results. *Ecology, Vol 67(4),* pp.919-928

Kitching, J.A. and Lockwood, J., 1974. Observations on shell form and its ecological significance in thaisid gastropods of the genus *Lepsiella* in New Zealand. *Marine Biology,Vol 28(2),* pp.131-144

Li, J. and Tao, D., 2012. On preserving original variables in Bayesian PCA with application to image analysis*. IEEE Transactions on Image Processing, Vol 21(12),* pp.4830-4843

MacLeod, N., 1999. Generalizing and extending the eigenshape method of shape space visualization and analysis*. Paleobiology, Vol 25(1),* pp.107-138

Morita, R., 1991. Mechanical constraints on aperture form in gastropods. *Journal of Morphology, Vol 207(1),* pp.93-102

Nakajima, S., Sugiyama, M. and Babacan, D., 2011. On Bayesian PCA: Automatic dimensionality selection and analytic solution. In: *Proceedings of the 28th International Conference on Machine Learning (ICML-11),* pp.497-504

Nounou, M.N., Bakshi, B.R., Goel, P.K. and Shen, X., 2002. Bayesian principal component analysis. *Journal of Chemometrics, 16(11),* pp.576-595

Oksanen, J., Kindt, R., Legendre, P., O'Hara, B., Stevens, M.H.H., Oksanen, M.J. and Suggests, M.A.S.S., 2007. The vegan package. *Community Ecology Package, Vol 10,* pp.631-637

Paliy, O. and Shankar, V., 2016. Application of multivariate statistical techniques in microbial ecology. *Molecular Ecology, Vol 25 (5),* pp.1032-1057

Pardo, L.M. and Johnson, L.E., 2004. Activity and shelter use of an intertidal snail: effects of sex, reproductive condition and tidal cycle. *Journal of Experimental Marine Biology and Ecology, Vol 301(2),* pp.175-191

Pearson, K., 1901. On lines and planes of closest fit to systems of points in space. *The London, Edinburgh, and Dublin Philosophical Magazine and Journal of Science, Vol 2(11),* pp.559-572

Queiroga, H., Costa, R., Leonardo, N., Soares, D. and Cleary, D.F., 2011. Morphometric variation in two intertidal littorinid gastropods. *Contributions to Zoology, Vol 80(3)*

Rabinowitz, G.B., 1975. An introduction to nonmetric multidimensional scaling. *American Journal of Political Science,* pp.343-390

Raup, D.M., 1961. The geometry of coiling in gastropods. *Proceedings of the National Academy of Sciences, Vol 47(4),* pp.602-609

Reid, D.G., 1996. Systematics and evolution of *Littorina* (No. 164). London: Ray Society

Reimchen, T.E., 1974. Studies on the biology and colour polymorphism of two sibling species of marine gastropod (*Littorina*). PhD dissertation, University of Liverpool, Liverpool

Rolan-Alvarez, E., Johannesson, K. and Erlandsson, J., 1997. The maintenance of a cline in the marine snail *Littorina saxatilis*: the role of home site advantage and hybrid fitness. *Evolution,* pp.1838-1847

Scheiner, S.M., 1993. Plasticity as a selectable trait: reply to Via. *The American Naturalist, Vol 142(2),* pp.371-373

Schindel, D.E., 1990. Unoccupied morphospace and the coiled geometry of gastropods: architectural constraint or geometric covariation? In: *Causes of evolution: a paleontological perspective.* Ross, R.M. and Allmon, W. D. (Eds). University of Chicago Press, Chicago, pp.270-304

Shimodaira, H., 2002. An approximately unbiased test of phylogenetic tree selection. *Systematic Biology, Vol 51,* pp.492-508

Shimodaira, H., 2004. Approximately unbiased tests of regions using multistep-multiscale boot-strap resampling. *Annals of Statistics, Vol 32,* pp.2616-2641

Smith, J.E., 1981. The natural history and taxonomy of shell variation in the periwinkles *Littorina saxatilis* and *Littorina rudis*. *Journal of the Marine Biological Association of the United Kingdom, Vol 61(1),* pp.215-241

Sundberg, P., 1988. Microgeographic variation in shell characters of *Littorina saxatilis* Olivi—a question mainly of size? *Biological Journal of the Linnean Society, Vol 35(2),* pp.169-184

Suzuki, R. and Shimodaira, H., 2004. An application of multiscale bootstrap resampling to hierarchical clustering of microarray data: How accurate are these clusters? *The Fifteenth International Conference on Genome Informatics,* P034

Suzuki, R. and Shimodaira, H., 2006. Pvclust: an R package for assessing the uncertainty in hierarchical clustering. *Bioinformatics, Vol 22(12),* pp.1540-1542

Takada, Y., 2003. Dimorphic migration, growth, and fecundity in a seasonally split population *of Littorina brevicula* (Mollusca: Gastropoda) on a boulder shore. *Population ecology, Vol 45(2),* pp.141-148

Thompson, D.W., 1942. On growth and form. Cambridge, Cambridge University Press

Tipping, M.E. and Bishop, C.M., 1999. Probabilistic principal component analysis. *Journal of the Royal Statistical Society: Series B (Statistical Methodology), Vol 61(3),* pp.611-622

Trussell, G.C., 1997. Phenotypic plasticity in the foot size of an intertidal snail. *Ecology, Vol 78(4),* pp.1033-1048

Trussell, G.C., 2000. Phenotypic clines, plasticity, and morphological trade-offs in an intertidal snail. *Evolution, Vol 54(1),* pp.151-166

Trussell, G.C., 2002. Evidence of countergradient variation in the growth of an intertidal snail in response to water velocity. *Marine Ecology Progress Series, Vol 243,* pp.123-131

Trussell, G.C., Johnson, A.S., Rudolph, S.G. and Gilfillan, E.S., 1993. Resistance to dislodgement: habitat and size-specific differences in morphology and tenacity in an intertidal snail. *Marine Ecology Progress Series,* pp.135-144

Vermeij, G.J. and Currey, J.D., 1980. Geographical variation in the strength of thaidid snail shells. *The Biological Bulletin, Vol 158(3),* pp.383-389

Vermeij, G.J., 1971. Gastropod evolution and morphological diversity in relation to shell geometry. *Journal of Zoology, Vol 163(1),* pp.15-23

Via, S., 1994. The evolution of phenotypic plasticity: what do we really know? *Ecological genetics*, pp.35-57

Walker, T.N. and Grahame, J.W., 2011. Shell shape variation and fitness variables in the gastropod *Littorina saxatilis*. *Marine Ecology Progress Series, Vol 430,* pp.103-111

Wentzell, P.D., Andrews, D.T., Hamilton, D.C., Faber, K. and Kowalski, B.R., 1997. Maximum likelihood principal component analysis. *Journal of Chemometrics, Vol 11(4),* pp.339-366

Wilding, C.S., Butlin, R.K. and Grahame, J., 2001. Differential gene exchange between parapatric morphs of *Littorina saxatilis* detected using AFLP markers. *Journal of Evolutionary Biology, Vol 14(4),* pp.611-619

WinkleStats. 2017. Boroka Kiss. [ONLINE] Available at: https://winklestats.wordpress.com/ [Accessed 23 April 2017]

Witman, J.D., 1985. Refuges, biological disturbance, and rocky subtidal community structure in New England. *Ecological monographs, Vol 55(4),* pp.421-445

Wold, S., 1994. Exponentially weighted moving principal components analysis and projections to latent structures. *Chemometrics and intelligent laboratory systems, Vol 23(1),* pp.149-161